Version of Record citation:

Raghupathi, R., Duffield, M. D., Zelkas, L., Meedeniya, A., Brookes, S. J. H., Sia, T. C., Wattchow, D. A., Spencer, N. J. and Keating, D. J. (2013), Identification of unique release kinetics of serotonin from guinea-pig and human enterochromaffin cells. The Journal of Physiology, 591: 5959–5975. doi: 10.1113/jphysiol.2013.259796

Serotonin release from guinea-pig and human enterochromaffin cells occurs with synaptic kinetics.

Ravinarayan Raghupathi[1], Michael D Duffield[1], Leah Zelkas[1], Adrian Meedeniya[3], Nick J Spencer[1,] Simon JH Brookes[1], Tiong Chen Sia[1,2], David A Wattchow[2], and Damien J Keating[1].

[1]Department of Human Physiology and Centre for Neuroscience and [2]Department of Surgery, Flinders University, Adelaide, 5001, Australia, [3]Eskitis Institute for Cell and Molecular Therapies, Griffith University, Gold Coast, 4111, Australia.

Abbreviated title: 5-HT release from primary enterochromaffin cells.

Corresponding author: Associate Professor Damien Keating, Department of Human Physiology and Centre for Neuroscience, Flinders University, Sturt Rd, Adelaide, Australia.
Ph: +61882044282, fax: +61882045768, email: damien.keating@flinders.edu.au

Number of pages: 33, figures: 6, tables: 2, movies: 3

Number of words in Abstract: 249, Introduction: 442, Discussion: 771

Conflict of Interest: The authors declare no competing financial interests.

Acknowledgements: This work is supported by an Australian Research Council Future Fellowship and Discovery Grant to DJK and a NHMRC Project grant (#10257566) to NJS. The authors would like to thank Melinda Kyloh and Sarah Nicholas for their technical assistance.

Abstract

The major source of serotonin (5-HT) in the body is the enterochromaffin (EC) cells lining the intestinal mucosa of the gastrointestinal tract. Despite the fact that EC cells synthesise ~95% of total body 5-HT, and that this 5-HT has important paracrine and endocrine roles, no studies have investigated the physiological function of single primary EC cells. We have developed a rapid primary culture of guinea pig and human EC cells, allowing analysis of single EC cell function using electrophysiology, electrochemistry, Ca^{2+} imaging, immunocytochemistry and 3D modelling. Ca^{2+} enters EC cells upon stimulation and triggers quantal 5-HT release via L-type Ca^{2+} channels. Real time amperometric techniques reveal that EC cells release 5-HT at rest and this release increases upon stimulation. Surprisingly for an endocrine cell storing 5-HT in large dense core vesicles (LDCVs), EC cells release 70 times less 5-HT per fusion event than catecholamine released from similarly sized LDCVs in endocrine chromaffin cells and the vesicle release kinetics instead resembles that observed in mammalian synapses. Furthermore, we measured EC cell density along the gastrointestinal tract to create three-dimensional simulations of 5-HT diffusion using the minimal number of variables required to understand the physiological relevance of single cell 5-HT release in the whole tissue milieu. These models indicate that local 5-HT levels are likely to be maintained around the activation threshold for mucosal 5-HT receptors and that this is dependent upon stimulation and location within the gastrointestinal tract. This is the first study demonstrating

single cell 5-HT release in primary EC cells. The mode of 5-HT release may represent a unique mode of exocytosis amongst endocrine cells and appears to be functionally relevant within the gastrointestinal tract.

Introduction

Enterochromaffin (EC) cells are enteroendocrine cells providing ~95% of total body 5-HT (Gershon and Tack, 2007). Enteroendocrine cells collectively represent the largest endocrine organ in our body and EC cells are the major enteroendocrine cell. Gut-derived 5-HT serves diverse endocrine roles in blood clotting, liver regeneration, bone formation (Karsenty and Gershon, 2011), embryo development (Cote et al., 2007), glucose homeostasis (Sumara et al., 2012) and the increased β-cell mass that prevents gestational diabetes (Kim et al., 2010). EC cell 5-HT also serves multiple paracrine roles in the gastrointestinal (GI) tract by activating secretory reflexes and modulating excitability of extrinsic sensory nerves (Gershon and Tack, 2007; Keating and Spencer, 2010; Spencer et al., 2011). EC cells respond to luminal stimuli including distension, acid and glucose to activate 5-HT_3 receptors on vagal mucosal afferent fibres (Blackshaw and Grundy, 1993; Lee et al., 2011). 5-HT_3 receptors antagonists are used clinically to reduce the nausea and vomiting caused by chemotherapy-induced surges in EC cell 5-HT release that activate mucosal vagal afferent fibres innervating the brainstem vomiting centres (Gershon and Tack, 2007).

Despite their importance however, primary EC cells have yet to be studied at the single cell level. Previous investigations of EC cells at the single cell level have utilised cell lines derived from pancreatic carcinomas (Kim et al., 2001; Braun et al., 2007) or the human small intestinal carcinoid-derived neoplasia (Kidd et al., 2007), but how closely their function represents primary EC cell function is questionable. Results from studies of primary EC cell function using whole tissue or isolated crypts (Lomax et al., 1999; Nozawa et al., 2009; Keating and Spencer, 2010) are

confounded by indirect effects from non-EC cells, such as neurons, epithelial cells and myocytes, in these preparations, or by gut wall contraction which is a major stimulus of EC cell 5-HT release (Keating and Spencer, 2010). While ELISA assays of 5-HT release from primary human EC cell cultures have recorded responses to a number of physiological stimuli (Kidd et al., 2008), no study has yet demonstrated the cellular mechanisms by which 5-HT is released from primary single EC cells.

The aims of this present study is to understand the mechanisms controlling the release of 5-HT from primary EC cells, and to compare these mechanisms between the human intestine; and a commonly studied animal model of GI function, the guinea-pig intestine; and compare these release mechanisms with release from other endocrine cells. We additionally have developed sophisticated three-dimensional models of the diffusion of 5-HT released from EC cell populations throughout the GI tract to understand what the implications of the EC cell release mechanisms would be for activation of 5-HT receptors located on mucosal nerve endings.

Materials & Methods

Primary culture and purification of guinea pig and human EC cells

Adult guinea pigs were killed humanely by stunning with a blow to the head followed by severing of the carotid arteries, as approved by the Flinders University Animal Welfare Committee. 4-6 cm of distal colon was removed and EC cell isolation and purification conducted using a modified approach from those previously published (Schafermeyer et al., 2004; Kidd et al., 2006). The mucosal layer of the colon was scraped off, minced and washed once in Buffer A ((mM): 140 NaCl, 5 KCl, 2 $CaCl_2$, 1 $MgCl_2$, 10 HEPES, 5 D-Glucose, pH7.4). The tissue was then digested in trypsin-EDTA (0.05%) with collagenase A (1 mg/ml, Roche Diagnostics, Germany) at 37°C for 30 min with continuous agitation. An equal volume of growth medium (DMEM containing 10% FBS, 1% L-glutamine and 1% penicillin-streptomycin) stopped this reaction. The suspension was filtered through a 40 µm steel mesh filter and centrifuged (Sigma, 6K15, USA) at 1000 x *g*. The resultant pellet was resuspended in 1ml of growth medium and layered onto a Percoll density gradient formed according to manufacturer's instructions. After centrifuging at 1100 x *g* for 8 min with slow braking, EC cells were harvested at a density of approximately 1.07 g/l, washed once with growth medium and plated onto 6 cm^2 pre-treated cell culture dishes (Iwaki, Australia). EC cells were maintained in growth medium for 2-4 days. All chemicals were from Sigma Aldrich, USA unless otherwise stated. Human colon tissue samples were obtained with prior informed consent from patients undergoing elective colectomy at the Flinders Medical Centre under the approval of the Southern Adelaide Clinical Human Research Ethics Committee. Cultures were obtained from 4 female patients aged 54-88 years old. Approximately 2 cm^2 of mucosa was dissected from areas of colon well removed from the site of tumours. This tissue was

processed as described above and EC cells plated and studied in the first 24h post-culture. EC cell viability was measured by incubating cells with Trypan blue (0.2% final concentration) for 5-10 min at 37°C followed by a cell count on a hemocytometer. Cells were considered viable if they completely excluded the dye. All results are from >3 separate cell cultures.

Immunocytochemical analysis of EC cell purification

EC cells were grown for 24h on glass cover slips previously coated with 10 µg/ml each of poly-D-lysine and laminin (Sigma-Aldrich, USA) in growth medium. Cells were fixed for 18-20h in Zamboni's fixative at 4°C followed by serial 5 min washes as follows: 4 x 80% EtOH, 2 x 100% EtOH, 3 x DMSO, 4 x PBS. Fixed cells were incubated for 30 min in 10% normal donkey serum diluted in antibody diluent (290 mM NaCl, 7.5 mM Na_2HPO_4, 2.6 mM Na_2HPO_4 $2H_2O$, 0.1% NaN_3 in distilled water, pH 7.1), followed by incubation for 24h in a humid chamber with goat monoclonal antibody against 5-HT (Jackson Immunoresearch, USA, 1:400) or sheep monoclonal antibody against TPH-1 (Millipore USA, Cat. No. AB1541, 1:200). After 3 washes with PBS, the cells were incubated with donkey anti-goat IgG or donkey anti-sheep IgG tagged with Cy3 (Jackson Immunoresearch, USA, 1:200 and DAPI (Sigma-Aldrich, USA, 1:500) for 2h in a humid chamber. Cells were then washed 3 times with PBS and the cover slips mounted onto glass slides in buffered glycerol. Fluorescence was visualised on a Leica TCS SP5 Spectral confocal microscope. The purity of the EC cell culture was calculated by assessing the proportion of DAPI-positive cells which were 5-HT-positive. Using this approach we calculated that the cells in these cultures were 98% 5-HT-positive.

Carbon fibre amperometric analysis of 5-HT release

Release of 5-HT from single EC cells was measured using carbon fibre amperometry (Keating et al., 2008). A carbon fibre electrode (ProCFE, Dagan Corporation, USA) was placed directly above an EC cell and +400mV applied to the electrode under voltage clamp conditions as this is the oxidation peak for 5-HT. Current due to 5-HT oxidation was recorded using an EPC-9 amplifier and Pulse software (HEKA Electronic, Germany) with the current sampled at 100 kHz and low-pass filtered at 3 kHz. For quantitative analysis files were converted to Axon Binary Files (ABF Utility, version 2.1, Synaptosoft, USA) and secretory spikes analysed (Mini Analysis, version 6.0.1, Synaptosoft, USA). The standard bath solution was Buffer A. High K^+-containing solution was the same as Buffer A except that 70 mM K^+ replaced an equimolar amount of NaCl. To analyse the effect of Ca^{2+} entry on 5-HT release, cells were exposed to 70 mM K^+ in the absence of external Ca^{2+}. All solutions were applied to cells using a gravity perfusion system at 34-37°C.

For recordings from EC cells, amperometric spikes were selected for analysis of event frequency if spike amplitude exceeded 10pA. For spike frequency calculations we counted spikes occurring within 60 sec of the start of stimulation. For kinetic analysis of spikes only those events that were not overlapping were included. Rise time of each spike was calculated from the 50–90% rising phase. Chromaffin cells and chromaffin cell amperometry data were obtained from adult mice as previously described (Zanin et al., 2011). All spikes that met our selection criteria were included in calculating the median values of each spike parameter for each recording. The averages of these median values were then used to compare each parameter

between cell populations (Colliver et al., 2001). This provides a parametric data set which was subsequently tested for statistical differences using an unpaired Student's t-test. For comparisons of spike kinetics in unstimulated and stimulated cells, we pooled all the spike data as we could not obtain a meaningful median value in many unstimulated cell recordings due to the low number of spikes. These data sets were compared using a Mann-Whitney test for non-parametric data sets. $p<0.05$ was taken as the lowest level of statistical significance. All data presented are shown as mean ± SEM and all data is from at least 3 different cell cultures.

Calcium imaging and Ca^{2+} currents

Changes in EC cell Ca^{2+} level were measured at 34–37°C using previously described methods (Zanin et al., 2011). Whole cell perforated patch clamp was performed using a EPC-10 patch clamp amplifier and PatchMaster software (HEKA Electronik, Lambrecht/Pfalz, Germany). Patch pipettes were pulled from borosilicate glass and fire polished, with resistance of 3-5 MΩ. Patch clamping was performed in the whole-cell configuration for measurement of Ca^{2+} currents, using an internal solution containing (mM): 135 Cs-Glutamate; 9 NaCl; 10 HEPES; 0.5 TEA-Cl; pH 7.2. External solution contained (mM): 150 NaCl; 2.8 KCl; 10 HEPES; 2 $MgCl_2$; 10 $CaCl_2$; 10 glucose; (pH 7.4). Calcium currents were elicited in the voltage-clamp mode using a voltage step protocol, in which voltage was stepped from a holding potential of -80 mV to voltages between -80 and 50 mV (10 mV increments) for 100ms. Series resistance was compensated at least 70%.

Calcium imaging

EC cells were treated with Fluo-4 (4μM) in serum-free DMEM for 30 min at 37°C. Cells were washed twice in Buffer A, which also served as the standard bath buffer.

Cells were stimulated for 60 sec with the same solution as Buffer A except that 70 mM K^+ replaced an equimolar amount of NaCl. and Ca^{2+} influx imaged as increases in cell fluorescence on a Cascade II fluorescence microscope (Photometrix USA). Results were analysed on Imaging Workbench software (version 6.0.22) (INDEC Systems, Inc, USA). All experiments were carried out at 34–37°C.

Measurements of EC cell density throughout the GI tract

Tissues from pre-selected regions of guinea pig gastrointestinal tract were dissected free and placed in Krebs solution (in mM: NaCl; 117, KCl; 5, $MgSO_4$; 1.2, $NaHCO_3$; 25; NaH_2PO_4, 1.2; $CaCl_2$; 2.5, Glucose; 10, bubbled with 95% O_2/ 5% CO_2, pH 7.4) containing 1µm nicardipine. Samples were taken from the mid-oesophagus (oesophagus) and the lower oesophageal sphincter region (cardia), the fundus, corpus and antrum of the stomach, the antral / pyloric border, the pyloric sphincter region and the duodenal / pyloric border, the mid-duodenum, the proximal, mid and distal ileum, the caecum, the proximal and distal colon and the rectum. The tissues were pinned on Sylgard blocks with maximal stretching and taken through the fixation, clearing and impregnation processes while pinned to these blocks. Tissue was fixed overnight in modified Zamboni's fixative (2% formaldehyde and 15% picric acid in 0.1M phosphate buffer, pH 7.0) and cleared in dimethyl sulphoxide (DMSO) for 30 minutes with the solution changed every 10 minutes. Samples were then dehydrated through an alcohol series comprising 50%, 70% and 95% ethanol for 15 minutes in each solution and in 100% ethanol for one hour. The tissues were then impregnated with polyethylene glycol (PEG, Sigma, NSW, Australia), by immersion in PEG 200 followed by PEG 400, for one hour in each solution at room temperature. The tissues were then placed in a solution of PEG 1000 for 60 minutes, *in vacuo*,

and with a desiccant (silica gel) at 45-48°C. The tissues were unpinned from the Sylgard blocks, trimmed, oriented in PEG 1400 in a cryo-mould and then embedded in PEG 1400 by hardening at -20 °C for five minutes, *in vacuo*. The blocks were sectioned at 60µm thickness on a rotary microtome at room temperature. The sections were placed on agarose (Sigma, NSW, Australia) sheets 3% in phosphate buffered saline (PBS) and the agarose sheets were placed on chrome alum slides with the sections contacting the slides. The slides, with the agarose sheets, were then dehydrated, *in vacuo*, with P_2O_5 for 20 minutes, placed in PBS on a rocker until the agarose sheets floated free, leaving the sections adhering to the slides. The slides were kept overnight, at room temperature in fresh PBS to further enhance the removal of the PEG from the sections.

Immunoreactivity for 5-HT was revealed by indirect immunofluorescence with sections incubated overnight in goat anti-5-HT (108072, 1:1000, Incstar) primary antibody in a humidified chamber. The primary antisera were visualised using CY3 conjugated donkey anti-goat IgG (Jackson, Pennsylvania, USA, code: 26035, 1:300). The tissues were incubated overnight with the secondary antibodies. The sections were then mounted in bicarbonate buffered glycerol and analysed. EC cells from each region were clearly identified by their immunoreactivity for 5-HT and counted in 3 guinea-pigs. A standard sample area of 200µm x 200µm was used for cell counts on a Vanox Olympus microscope fitted with epifluorescence. Images were processed using Image J (Bethesda, Maryland, USA). Sample areas were taken from all levels in the mucosa, oriented to exclude muscularis mucosa or regions that lacked tissue. 10 random samples were taken from each area, from each animal and cell density per unit volume of tissue calculated in each region. Using a section

thickness approximately twelve times the diameter of the EC cells and accurately defining cell morphology minimised sampling errors (Coggeshall and Lekan, 1996).

Simulation model

An explicit finite-differences model (described in more detail below), incorporating release of serotonin from EC cells, diffusion of serotonin, and uptake of serotonin by the SERT was used to simulated 5HT concentrations within the mucosa of different GIT regions.

Single cell models:

Single cell release models were of dimensions 50μm per side, discretised in 1μm steps (see equations below: $\Delta x, \Delta y, \Delta z = 1\mu m$), with the entire volume representing the mucosa layer, and with a single release site at the centre of the volume. This system was simulated for a sufficient amount of time for numerous release events to occur.

Tissue models:

Tissue models consisted of a cuboid region of dimensions between 400-1000μm per side, discretised in 10μm steps (see equations below: $\Delta x, \Delta y, \Delta z = 10\mu m$). For these models a mucosa cell was assumed to be of dimensions 10μm×10μm×10μm, consistent with the approximate measured dimensions of single EC cells. A cuboid layer representing mucosal tissue, of an appropriate thickness for the GIT region being modelled, was placed within this volume, with a submucosal layer 'below' and luminal layer 'above'. 5HT release points were randomly distributed throughout the mucosal layer at a density consistent with the experimentally determined EC cell density. 5HT entry and movement into the submucosal and luminal regions was

purely diffusional, with no release sites placed within these regions. To determine steady-state 5HT concentrations in the mucosa of different GIT regions stimulated or non-stimulated conditions models were run with a starting 5HT concentration of 0M at all points and allowed to run until the average mucosal concentration of 5HT had stabilised using event frequencies obtained from our own experiments in EC cells.

Contraction models:

To model the effects of GIT contraction it was assumed that contraction of the tissue would result in a change in EC cell state from 'unstimulated' to 'stimulated', with a resultant change in 5HT release rate, and the reverse during relaxation (Spencer et al., 2011). Therefore modelling of this process consisted of changing the 5HT release parameters at a rate consistent with the contraction/relaxation rate described experimentally (Table 1). These models were initially run in the 'relaxed' (non-stimulated release) state until steady-state had been achieved, at which point a series of contraction and relaxation events were simulated.

Model parameters:

Parameters utilised for the modelling are shown in Table 1, and are all based on experimentally determined parameters from the literature. The effective diffusion coefficient for 5HT in tissue was calculated based on the 5HT diffusion in CNS tissue, which found a tortuosity constant of 1.65 for 5HT (representing an effective diffusion coefficient in tissue approximately 3x smaller than that in aqueous solution). This effective tissue diffusion constant was used for the mucosal and submucosal layers of the model, whilst diffusion within the luminal layer utilised a diffusion coefficient consistent with that reported for 5HT in aqueous solution.

Models were written in the Python programming language (www.python.org), utilising the NumPy/SciPy libraries (Jones et al., 2001).

Model derivation

The diffusion (or heat) equation for a 3 dimensional system is:

$$\frac{\partial u}{\partial t} = D\left(\frac{\partial^2 u}{\partial x^2} + \frac{\partial^2 u}{\partial y^2} + \frac{\partial^2 u}{\partial z^2}\right)$$

Where:

$u(x, y, z, t)$

$x, y, z, t \in \mathbb{R}$

Describes the concentration of 5HT at position *(x,y,z)* and time, *t*

And:

D is the diffusion coefficient

This equation can be extended to incorporate chemical source(s)/sink(s):

$$\frac{\partial u}{\partial t} = D\left(\frac{\partial^2 u}{\partial x^2} + \frac{\partial^2 u}{\partial y^2} + \frac{\partial^2 u}{\partial z^2}\right) + g(x, y, z, t)$$

Where:

$g(x, y, z, t)$

Gives the concentration of chemical added to point (x,y,z) and time, t

We have solved this system numerically using an explicit finite differences model, where the approximate solution at the grid points is given by:

$$u_{i,j,k}^{m} \equiv u(x_i, y_j, z_k, t_m)$$

In brief, the domain was discretised in x,y,z and t:

$$x_i = x_0 + i\Delta x$$

$$y_j = y_0 + j\Delta y$$

$$z_k = z_0 + k\Delta x$$

$$t_m = t_0 + m\Delta t$$

$$i, j, k, m \in \mathbb{Z}$$

and the derivatives expressed in terms of finite differences (using a forward difference for $\frac{\partial u}{\partial t}$, and a central difference for $\frac{\partial^2 u}{\partial x^2}$, $\frac{\partial^2 u}{\partial y^2}$ and $\frac{\partial^2 u}{\partial z^2}$, such that:

$$\frac{\partial u}{\partial t} = \frac{u_{i,j,k}^{m+1} - u_{i,j,k}^{m}}{\Delta t} + O(\Delta t)$$

And:

$$\frac{\partial^2 u}{\partial x^2} = \frac{u_{i+1,j,k}^{m} - 2u_{i,j,k}^{m} + u_{i-1,j,k}^{m}}{(\Delta x^2)} + O(\Delta x^2)$$

Likewise for $\frac{\partial^2 u}{\partial y^2}$ and $\frac{\partial^2 u}{\partial z^2}$

Substituting into:

$$\frac{u_{i,j,k}^{m+1} - u_{i,j,k}^{m}}{\Delta t} = D\left(\frac{u_{i+1,j,k}^{m} - 2u_{i,j,k}^{m} + u_{i-1,j,k}^{m}}{(\Delta x)^2} + \frac{u_{i,j+1,k}^{m} - 2u_{i,j,k}^{m} + u_{i,j-1,k}^{m}}{(\Delta y)^2} + \frac{u_{i,j,k+1}^{m} - 2u_{i,j,k}^{m} + u_{i,j,k-1}^{m}}{(\Delta z)^2}\right) + g_{i,j,k}^{m}$$

Solving for $u_{i,j,k}^{m+1}$ then gives us:

$$u_{i,j,k}^{m+1} = u_{i,j,k}^{m} + D\Delta t\left(\frac{u_{i+1,j,k}^{m} - 2u_{i,j,k}^{m} + u_{i-1,j,k}^{m}}{(\Delta x)^2} + \frac{u_{i,j+1,k}^{m} - 2u_{i,j,k}^{m} + u_{i,j-1,k}^{m}}{(\Delta y)^2} + \frac{u_{i,j,k+1}^{m} - 2u_{i,j,k}^{m} + u_{i,j,k-1}^{m}}{(\Delta z)^2}\right) + \Delta t g_{i,j,k}^{m}$$

Stability

The explicit finite difference model described above is conditionally stable, providing that:

$$D\Delta t\left(\frac{1}{\Delta x^2} + \frac{1}{\Delta y^2} + \frac{1}{\Delta z^2}\right) \leq \frac{1}{2}$$

In all models the spatial discretization parameters $\Delta x^2, \Delta y^2 \Delta z^2$ were determined as described previously, and then the time discretisation, Δt, determined to ensure that this condition was fulfilled at all times.

SERT Uptake

Uptake by the SERT transporter was modelled as a Michaelis-Menten process:

$$\frac{du}{dt} = \frac{V_{max} u}{K_m + u}$$

Where V_{max} is the SERT uptake rate at saturating 5HT concentrations and K_m is the Michaelis constant for the SERT transporter

5HT release

5HT release was modelled as a Poisson process:

$$P\left[\left(N(t+\Delta t)-N(t)\right)=k\right]=\frac{e^{-\lambda\Delta t}(\lambda\Delta t)^{k}}{k!}$$

Where:

$k \in \mathbb{N}^0$

$\left(N(t+\Delta t)-N(t)\right)=k$ is the number of events in the time interval $(t, t+\Delta t]$

With rate parameter λ representing the expected number of release events per unit time.

Statistical analysis

All data are presented as mean ± SEM. Error bars represent SEM. Analyses of significant differences between means were performed using two-tailed Student's t tests or Mann-Whitney test when comparing two groups of parametric or non-parametric data sets. n, number of independent cultures or animals used. In all cases, *p < 0.05, **p < 0.01, ***p < 0.001.

Results

Isolation and purification of EC cells

We purified EC cells from guinea pig colon and maintained them in primary culture (Figure 1A). Immunolabelling confirmed these cells as 5-HT-containing EC cells (Figure 1B) with a purity of >98% (Figure 1C). 5-HT expression in the cytoplasm is punctate (Figure 1D) and these cells also contain Tph1 (Figure 1E), further confirming them as EC cells. Cell viability was >98% for the first 48 hours in culture (Figure 1F).

Stimulation of purified primary EC cells causes Ca^{2+} entry and 5-HT release

Whole cell patch clamp demonstrated voltage-gated Ca^{2+} channels in EC cells (Figure 2A) which peak at 20-30mV (Figure 2B). Ca^{2+} imaging in cells loaded with Fluo-4 demonstrated that membrane depolarisation with either 70mM K^+ or acetylcholine (10μM) induced Ca^{2+} entry (Figure 2C). Thus, EC cell stimulation causes the entry of Ca^{2+}, the main physiological trigger of secretion. We then used carbon fibre amperometry to measure 5-HT release from single EC cells. Carbon fibre probes were held at the oxidation peak for 5-HT, +400mV (Figure 2E, *inset*) and placed adjacent to a single EC cell. Individual amperometric peaks indicative of single vesicle release of 5-HT were observed under basal and stimulatory (70mM K^+) conditions (Figure 2D). Similar results were observed with acetylcholine (10μM, Figure 3D). To confirm our oxidation currents represented 5-HT release, we incubated EC cells for 24 hours with an inhibitor of Tph, LP533401 (1μM, Dalton USA), which results in almost complete suppression of 5-HT synthesis (Yadav et al., 2010). These cells (Figure 2E) showed significantly reduced release (Figure 2F,

p<0.001), confirming that these oxidation peaks represent single 5-HT release events from primary EC cells.

EC cell 5-HT release is dependent on external Ca^{2+} entry through L-type Ca^{2+} channels

A reduced number of 5-HT release events were observed when EC cells were stimulated in absence of external Ca^{2+} (Figure 2A and B). Blocking L-type Ca^{2+} channels with nicardipine (2μM) also reduced release event frequency (Figure 2C). Thus, 5-HT release from EC cells is largely dependent on Ca^{2+} entry with one major avenue being through L-type Ca^{2+} channels (Figure 2D).

Single 5-HT release events occur with rapid kinetics in EC cells

Individual current peaks in amperometric recordings represent the release of oxidizable substances from a single vesicle (Figure 4A). Vesicle size is a major determinant of vesicle release kinetics (Albillos et al., 1997; Zhang and Jackson, 2010) so we compared single EC cell events to those in the more commonly studied endocrine cell, the adrenal chromaffin cell (Figure 4B), which release catecholamines from similarly sized large dense core vesicles (LDCVs) (Nilsson et al., 1987; Pothos et al., 2002). This comparison demonstrates the amount released per exocytosis event was much smaller in EC cells (Figure 4C). Comparisons of frequency distribution of spike width at half maximum height (half-width, Figure 4D), rise time (Figure 4E) and decay-time (Figure 4F) further confirmed the lack of overlap between these groups. Unexpectedly, the amount of 5-HT released per fusion event was similar to that seen for release of dopamine from much smaller synaptic vesicles (Staal et al., 2004) (Table 2).

The 5-HT release profile in human and guinea-pig EC cells is identical

We also isolated and cultured human colonic EC cells and measured single 5-HT release events (Figure 5A). Spike frequency in unstimulated and stimulated cells (Figure 5B) was similar to that in guinea pig. The relative number of release events over time was identical in human and guinea pig EC cells, and was significantly reduced in the absence of external Ca^{2+} or when L-type Ca^{2+} channels were blocked (Figure 5C). Single exocytosis events also occurred in human EC cells (Figure 5D) and the distribution of spike area was strikingly similar to guinea pig EC cells (Figure 5E). To test whether partial release via kiss and run fusion might explain the synaptic-like kinetics of 5-HT release in EC cells we inhibited Tph activity for 24 hours with LPS533401 (1μM) to reduce the availability of 5-HT to be loaded into vesicles. If EC cell vesicles release 5-HT via full fusion, this treatment would result in reduced spike charge (Colliver et al., 2000; Pothos et al., 2002; Gong et al., 2003; Sombers et al., 2004). The mean charge of release events was unaltered by this treatment (Figure 5F), indicating that rapid kiss and run, rather than full fusion, may be occurring in EC cells and may explain these rapid release kinetics and low amounts of 5-HT release per fusion event.

Relevance of EC cell release kinetics for 5-HT signalling

To gauge the physiological relevance of synaptic-like release of 5-HT from EC cells within the surrounding mucosal area, we modelled the three-dimensional diffusion of 5-HT throughout the surrounding tissue in different GI tract regions. This is important to try and relate the synaptic-like amounts of 5-HT released from EC cells with the local concentrations this would create and the relevance this has to the activation

threshold of 5-HT receptors present on mucosal nerve endings. We first quantified EC cell density in different gut regions. EC cells were rarely present in the oesophagus but were found at varying densities in the cardia, fundus, pylorus, ileum and colon, with the highest EC cell density in the pylorus (Figure 6A-G). We then modelled the diffusion of 5-HT released from a single cell to demonstrate the effect of stimulation on diffusion distance (Figure 6H). Using a more complex multi-cell simulation, we demonstrated that the steady state 5-HT levels differ in unstimulated and stimulated conditions in different GI tract regions when moving from a starting point of no 5-HT (Figure 6I). This can be better demonstrated however when viewing three dimensional (Figure 6J), vertical (Figure 6K) and horizontal (Figure 6L) plane as a still image or movie (Movie 1). Such analysis revealed regional differences in steady state 5-HT under stimulated and unstimulated conditions (Figure 6M). The modelling identified the probability of any space being exposed to 5-HT levels above 1nM (Figure 6N), which is close to the K_d for 5-HT binding to 5-HT receptors in mucosa-submucosa membrane preparations (Branchek et al., 1984). Modelling the 5-HT fluctuations that occur at resting contraction rates (Spencer et al., 2011) resulted in rapid changes in 5-HT levels across this K_d value (Figure 6O and Movie 2). At higher stimulation frequencies, 5-HT levels remained above this 1nM threshold (Figure 6P and Movie 3). Thus our models simulating diffusion of 5-HT from populations of EC cells in the mucosa reveal that the amount released per vesicle from EC cells may have physiological relevance. We find that local 5-HT levels depend on EC cell density and release frequency and that these 5-HT levels are very close to the activation threshold of innervating 5-HT receptors and that this threshold may be crossed during GI tract contraction or peristalsis.

Discussion

This represents the first study of single primary enterochromaffin cell function in any species. Whilst these cells constitute the most prevalent enteroendocrine cell within our largest endocrine tissue, they remain poorly understood. We demonstrate that EC cells contain voltage-gated Ca^{2+} channels, that Ca^{2+} enters EC cells upon stimulation, and that Ca^{2+} entry through L-type Ca^{2+} channels contributes significantly to 5-HT release. Most intriguingly, both guinea pig and human EC cells release an amount of 5-HT per exocytosis event equivalent to that seen in synaptic release. The amount of 5-HT released per fusion event appears to have physiological relevance in relation to activation of 5-HT receptors within the intestinal mucosa, with modelling of this type of release revealing that different GI tract regions are likely to be exposed to quite variable 5-HT levels within the mucosa.

We have developed a method of rapidly purifying and culturing EC cells from both guinea pig and human colonic mucosa. Previous methods for EC cell isolation have included using acridine orange staining followed by FACS sorting {Kidd, 2006 #1766} or elutriation and density gradient centrifugation {Schafermeyer, 2004 #1544}. Our approach was modified from that of {Schafermeyer, 2004 #1544} as we felt a brief enzyme digestion followed by density centrifugation is rapid and more likely to result in single cells healthy enough to allow measurements using sensitive techniques such as whole cell patch clamp. We have therefore been able to undertake the first single cell measurements of these important endocrine cells. Our results demonstrate that EC cells behave similarly to many other endocrine cells; they contain voltage-gated Ca^{2+} channels, they undergo exocytosis and release vesicle contents in a quantal manner, and this exocytosis is Ca^{2+}-dependent. We also find

that L-type Ca^{2+} channels contribute to a large proportion of secretion. This is similar to previous findings in isolated guinea pig and human duodenal crypts {Lomax, 1999 #1774}.

We do, however, observe one significant difference in the secretion profile of EC cells compared to other endocrine cells. Our amperometry experiments clearly demonstrate that EC cells release far less 5-HT per vesicle fusion event than that released from other cells containing similarly sized vesicles, such as adrenal chromaffin cells. Vesicle size is a significant factor underlying the different release kinetics of LDCVs and synaptic vesicles (Bruns et al., 2000), with the amount released per vesicle being proportional to vesicle size (Albillos et al., 1997; Zhang and Jackson, 2010). 5-HT is stored in guinea-pig EC cell LDCVs (Nilsson et al., 1987; Cetin et al., 1994; Fujimiya et al., 1997) of similar size to chromaffin cell LDCVs (Pothos et al., 2002; Zanin et al., 2012) however our data reveals that 70 times less 5-HT is released from EC cell vesicles than catecholamine released from chromaffin vesicles during each exocytosis event. The mechanisms underlying such a difference are unknown. Amperometric spikes recorded from chromaffin cells represent full fusion events, with transient “kiss and run” fusion measured as stand-alone foot signals in these cells. EC cell vesicles may be undergoing full fusion but such vesicles may contain comparatively small amounts of 5-HT per vesicle. This could potentially be due to differences in vesicular pH (Pothos et al., 2002) or VMAT expression to reduce 5-HT loading into EC cell vesicles. Alternatively, only the smallest LDCVs might undergo exocytosis in EC cells, although the mechanism that would govern such a pathway is unclear. Another explanation for this type of release in EC cells may be the exclusive occurrence of “kiss and run” fusion in which

transient pore opening and rapid re-closure results in only partial release of 5-HT. Indeed, immunoelectron micrographs of rat duodenal EC cells stimulated by increased intraluminal pressure demonstrates LDCVs that have only partially released their contents {Fujimiya, 1997 #2015}, possibly via kiss and run type fusion. This would be in line with our experiments in which inhibition of 5-HT synthesis, which should reduce 5-HT loading into individual vesicles, did not reduce quantal size as is observed in chromaffin cells when vesicle loading is inhibited. As this study is the first of its kind in EC cells, or indeed in any cell type derived from gastric stem cells (in contrast to the large amount of study undertaken in neural crest derived endocrine and neuroendocrine cells), it is also worth considering that previously undescribed mechanisms may control 5-HT release from EC cells. What we can be certain of is that this release mode is consistent between guinea pig and human EC cells, with the same amount of 5-HT released per fusion event in both species.

To try and understand the physiological relevance of the relatively small amounts of 5-HT released per fusion event in EC cells we created mathematical models to simulate 5-HT diffusion in the mucosal layer. 5-HT released from these cells has three major targets; 5-HT receptors located on intrinsic and extrinsic nerve endings, the serotonin transporters (SERT) located on enterocytes, and SERT located on local blood vessels for transport into the circulation {Chen, 2001 #2022}. 5-HT receptors can be saturated and desensitised by prolonged exposure to activating 5-HT concentrations. We therefore used the Kd value for 5-HT receptors located within mucosa-submucosa membrane preparations (~1nM) (Branchek et al., 1984) as a reference point to determine the ramifications of the synaptic-like amounts of 5-HT released during EC cell fusion events. Our three dimensional modelling of 5-HT

diffusion indicates that the amounts of 5-HT released would be sufficient to activate 5-HT receptors within relevant distances of secreting EC cells. We began with a model consisting of a single releasing cell in an empty volume secreting 5-HT with the same kinetics measured in our amperometric recordings. At this single cell level our model predicts that the 5-HT concentration remains above 1nM within 3μm of the release site in non-stimulated conditions, and within 7μm of the release site at a release frequency consistent with EC cell stimulation. While the number of close contacts between EC cells and other structures is low due to the constant migration of EC cells (O'Hara and Sharkey, 2007), nerve terminals are observed within these distances from EC cells (Wade and Westfall, 1985; Gershon and Tack, 2007). Such pathways are functional with, for example, mucosal 5-HT acting on vagal mucosal afferent fibres via 5-HT_3 receptors to control sensory pathways in response to luminal stimuli such as distension and acid (Blackshaw and Grundy, 1993).

We then used our modelling approach to identify the relevance of the 5-HT release profile from multiple EC cells within the mucosal layer itself. To do this required knowledge of EC cell density within various regions of the GI tract. We observe varying EC cell densities throughout the gut, with the highest density within the pylorus. Modelling of 5-HT diffusion from multiple EC cell populations within the mucosal layer indicates, as expected, that mucosal 5-HT concentrations would vary in accordance with EC cell density and stimulation status. Consequently, 5-HT receptors in these different areas of the gut may be differentially activated under resting and stimulated conditions, possibly leading to regional differences in receptor activation and desensitisation. It is also possible that the small amount of 5-HT released from EC cells may minimise desensitisation of local 5-HT receptors. Even

within those regions of the mucosa containing lower 5-HT concentrations, our single cell models predict that physiologically relevant 5-HT levels will still be present within a short distance of EC cells, and hence be relevant to receptors located within such proximity. Additionally, our models predict the existence of “hotspots” of high 5-HT concentration in discrete regions of the mucosa, whose functional significance is not yet clear. We speculate that these differences in cell density could underpin varying roles of EC cell 5-HT in different gut regions.

Interestingly our modelling, along with single cell ELISA values obtained from human EC cells {Kidd, 2008 #2007} demonstrates a disparity in the 5-HT concentrations obtained from cultured EC cells to those obtained with amperometry in whole tissue preparations. We predict average mucosal 5-HT concentrations in the nM range, similar to ELISA measurements from normal and neoplastic human EC cells {Kidd, 2008 #2007}. Our single cell data is also in line with ELISA measurements of 5-HT release from whole tissue that estimates 5-HT release in the pM 5-HT/g tissue range {Bertrand, 2010 #1504}. However measurement of 5-HT release from whole tissue, obtained with electrodes calibrated using constant-voltage amperometry in our laboratory and others {Bertrand, 2004 #1566;Bertrand, 2006 #1575;Bertrand, 2010 #1504;Keating, 2010 #1680;Spencer, 2011 #1749}, provide measurements of average mucosal 5-HT concentrations several orders of magnitude higher. Given that 5-HT levels in the mM range are expected to desensitise local receptors that are activated at nM levels, such concentrations make little sense in relation to their effect on 5-HT receptor activation. There may be several explanations that contribute to such a difference in estimates of EC cell 5-HT release. Firstly, the use of constant-voltage amperometry creates an artificial diffusion gradient toward the electrode that

will lead to overestimates of an unknown magnitude of the measured 5-HT concentration. Secondly, whole tissue recordings are more prone to probe fouling and reduction in electrode sensitivity during long recordings compared to single cell recordings. Thirdly, recordings in intact tissue measure luminal 5-HT release and maintaining EC cells in culture may cause them to lose any secretory polarity that might exist *in vivo* and as such affect the comparison being made between *in situ* vs. *in vitro* measurements. Additionally, *in situ* measurements of 5-HT release are likely triggered via mechanosensitive pathways in response to either gut contraction {Keating, 2010 #1680;Spencer, 2011 #1749} or probing with an amperometry electrode {Bertrand, 2004 #1566;Bertrand, 2006 #1575;Bertrand, 2010 #1504}. This type of stimulus may initiate far greater levels of 5-HT release than high external K^+ or acetylcholine used in our study. We also cannot be sure how many EC cells are located within the vicinity of an amperometry electrode during whole tissue amperometry experiments. As such, the use of fixed amperometry measurements of 5-HT concentrations in whole tissue preparations may overestimate the amount of 5-HT released from EC cells.

Our rapid EC cell isolation approach can be used to compare EC cell function in normal and pathological conditions in both human samples and animal models of GI disorders. This would have benefit over whole tissue measurements that can be confounded by indirect effects on EC cells from other surrounding cell types or by contraction of the GI tract. Our approach will hopefully underpin a new wave of investigations into the precise function and role of these endocrine cells in health and disease. As EC cell-derived 5-HT has important paracrine effects within the gut as well as endocrine effects on tissues including bone, liver and lung (Karsenty and

Gershon, 2011), such studies would have relevance both within the GI tract and beyond.

References

Albillos A, Dernick G, Horstmann H, Almers W, Alvarez de Toledo G, Lindau M (1997) The exocytotic event in chromaffin cells revealed by patch amperometry. Nature 389:509-512.

Blackshaw LA, Grundy D (1993) Effects of 5-hydroxytryptamine on discharge of vagal mucosal afferent fibres from the upper gastrointestinal tract of the ferret. J Auton Nerv Syst 45:41-50.

Branchek T, Kates M, Gershon MD (1984) Enteric receptors for 5-hydroxytryptamine. Brain Res 324:107-118.

Braun T, Voland P, Kunz L, Prinz C, Gratzl M (2007) Enterochromaffin cells of the human gut: sensors for spices and odorants. Gastroenterology 132:1890-1901.

Bruns D, Riedel D, Klingauf J, Jahn R (2000) Quantal release of serotonin. Neuron 28:205-220.

Cetin Y, Kuhn M, Kulaksiz H, Adermann K, Bargsten G, Grube D, Forssmann WG (1994) Enterochromaffin cells of the digestive system: cellular source of guanylin, a guanylate cyclase-activating peptide. Proc Natl Acad Sci U S A 91:2935-2939.

Coggeshall RE, Lekan HA (1996) Methods for determining numbers of cells and synapses: a case for more uniform standards of review. J Comp Neurol 364:6-15.

Colliver TL, Hess EJ, Ewing AG (2001) Amperometric analysis of exocytosis at chromaffin cells from genetically distinct mice. Journal of Neuroscience Methods 105:95-103.

Colliver TL, Pyott SJ, Achalabun M, Ewing AG (2000) VMAT-Mediated changes in quantal size and vesicular volume. Journal of Neuroscience 20:5276-5282.

Cote F, Fligny C, Bayard E, Launay JM, Gershon MD, Mallet J, Vodjdani G (2007) Maternal serotonin is crucial for murine embryonic development. Proc Natl Acad Sci U S A 104:329-334.

Fujimiya M, Okumiya K, Kuwahara A (1997) Immunoelectron microscopic study of the luminal release of serotonin from rat enterochromaffin cells induced by high intraluminal pressure. Histochem Cell Biol 108:105-113.

Gerhardt G, Adams RN (1982) Determination of diffusion coefficients by flow injection analysis. Analytical Chemistry 54:2618-2620.

Gershon MD, Tack J (2007) The serotonin signaling system: from basic understanding to drug development for functional GI disorders. Gastroenterology 132:397-414.

Gong LW, Hafez I, Alvarez de Toledo G, Lindau M (2003) Secretory vesicles membrane area is regulated in tandem with quantal size in chromaffin cells. J Neurosci 23:7917-7921.

Jones E, Oliphant T, Peterson P, others (2001) SciPy: Open Source Scientific Tools for Python. In.

Karsenty G, Gershon MD (2011) The importance of the gastrointestinal tract in the control of bone mass accrual. Gastroenterology 141:439-442.

Keating DJ, Spencer NJ (2010) Release of 5-hydroxytryptamine from the mucosa is not required for the generation or propagation of colonic migrating motor complexes. Gastroenterology 138:659-670.

Keating DJ, Dubach D, Zanin MP, Yu Y, Martin K, Zhao YF, Chen C, Porta S, Arbones ML, Mittaz L, Pritchard MA (2008) DSCR1/RCAN1 regulates vesicle exocytosis and fusion pore kinetics: implications for Down syndrome and Alzheimer's disease. Human Molecular Genetics 17:1020-1030.

Kidd M, Modlin IM, Eick GN, Champaneria MC (2006) Isolation, functional characterization, and transcriptome of Mastomys ileal enterochromaffin cells. Am J Physiol Gastrointest Liver Physiol 291:G778-791.

Kidd M, Eick GN, Modlin IM, Pfragner R, Champaneria MC, Murren J (2007) Further delineation of the continuous human neoplastic enterochromaffin cell line, KRJ-I, and the inhibitory effects of lanreotide and rapamycin. J Mol Endocrinol 38:181-192.

Kidd M, Modlin IM, Gustafsson BI, Drozdov I, Hauso O, Pfragner R (2008) Luminal regulation of normal and neoplastic human EC cell serotonin release is mediated by bile salts, amines, tastants, and olfactants. Am J Physiol Gastrointest Liver Physiol 295:G260-272.

Kim H, Toyofuku Y, Lynn FC, Chak E, Uchida T, Mizukami H, Fujitani Y, Kawamori R, Miyatsuka T, Kosaka Y, Yang K, Honig G, van der Hart M, Kishimoto N, Wang J, Yagihashi S, Tecott LH, Watada H, German MS (2010) Serotonin regulates pancreatic beta cell mass during pregnancy. Nat Med 16:804-808.

Kim M, Cooke HJ, Javed NH, Carey HV, Christofi F, Raybould HE (2001) D-glucose releases 5-hydroxytryptamine from human BON cells as a model of enterochromaffin cells. Gastroenterology 121:1400-1406.

Lee J, Cummings BP, Martin E, Sharp JW, Graham JL, Stanhope KL, Havel PJ, Raybould HE (2011) Glucose-sensing by Gut Endocrine Cells and Activation of the Vagal Afferent Pathway is Impaired in a Rodent Model of Type 2 Diabetes Mellitus. Am J Physiol Regul Integr Comp Physiol.

Lomax RB, Gallego S, Novalbos J, Garcia AG, Warhurst G (1999) L-Type calcium channels in enterochromaffin cells from guinea pig and human duodenal crypts: an in situ study. Gastroenterology 117:1363-1369.

Miller GM, Yatin SM, De La Garza R, 2nd, Goulet M, Madras BK (2001) Cloning of dopamine, norepinephrine and serotonin transporters from monkey brain: relevance to cocaine sensitivity. Brain Res Mol Brain Res 87:124-143.

Nilsson O, Dahlstrom A, Geffard M, Ahlman H, Ericson LE (1987) An improved immunocytochemical method for subcellular localization of serotonin in rat enterochromaffin cells. J Histochem Cytochem 35:319-326.

Nozawa K, Kawabata-Shoda E, Doihara H, Kojima R, Okada H, Mochizuki S, Sano Y, Inamura K, Matsushime H, Koizumi T, Yokoyama T, Ito H (2009) TRPA1 regulates gastrointestinal motility through serotonin release from enterochromaffin cells. Proc Natl Acad Sci U S A 106:3408-3413.

O'Hara JR, Sharkey KA (2007) Proliferative capacity of enterochromaffin cells in guinea-pigs with experimental ileitis. Cell Tissue Res 329:433-441.

Pothos EN, Mosharov E, Liu KP, Setlik W, Haburcak M, Baldini G, Gershon MD, Tamir H, Sulzer D (2002) Stimulation-dependent regulation of the pH, volume and quantal size of bovine and rodent secretory vesicles. Journal of Physiology 542:453-476.

Rice ME, Nicholson C (1986) Serotonin Migration in the Neuronal Microenvironment. Annals of the New York Academy of Sciences 481:381-382.

Schafermeyer A, Gratzl M, Rad R, Dossumbekova A, Sachs G, Prinz C (2004) Isolation and receptor profiling of ileal enterochromaffin cells. Acta Physiol Scand 182:53-62.

Sombers LA, Hanchar HJ, Colliver TL, Wittenberg N, Cans A, Arbault S, Amatore C, Ewing AG (2004) The effects of vesicular volume on secretion through the fusion pore in exocytotic release from PC12 cells. J Neurosci 24:303-309.

Spencer NJ, Nicholas SJ, Robinson L, Kyloh M, Flack N, Brookes SJ, Zagorodnyuk VP, Keating DJ (2011) Mechanisms underlying distension-evoked peristalsis in guinea pig distal colon: is there a role for enterochromaffin cells? Am J Physiol Gastrointest Liver Physiol 301:G519-527.

Staal RG, Mosharov EV, Sulzer D (2004) Dopamine neurons release transmitter via a flickering fusion pore. Nat Neurosci 7:341-346.

Sumara G, Sumara O, Kim JK, Karsenty G (2012) Gut-derived serotonin is a multifunctional determinant to fasting adaptation. Cell Metab 16:588-600.

Wade PR, Westfall JA (1985) Ultrastructure of enterochromaffin cells and associated neural and vascular elements in the mouse duodenum. Cell Tissue Res 241:557-563.

Yadav VK, Balaji S, Suresh PS, Liu XS, Lu X, Li Z, Guo XE, Mann JJ, Balapure AK, Gershon MD, Medhamurthy R, Vidal M, Karsenty G, Ducy P (2010) Pharmacological inhibition of gut-derived serotonin synthesis is a potential bone anabolic treatment for osteoporosis. Nat Med 16:308-312.

Zanin MP, Phillips L, Mackenzie KD, Keating DJ (2011) Aging differentially affects multiple aspects of vesicle fusion kinetics. PLoS One 6:e27820.

Zanin MP, Mackenzie KD, Peiris H, Pritchard MA, Keating DJ (2012) RCAN1 regulates vesicle recycling and quantal release kinetics via effects on calcineurin activity. J Neurochem.

Zhang Z, Jackson MB (2010) Membrane bending energy and fusion pore kinetics in Ca(2+)-triggered exocytosis. Biophys J 98:2524-2534.

Model Parameter	Value	Reference
EC cell vesicle release rate parameter (λ) (stimulated)	2.007 /s	Current paper
EC cell vesicle release rate parameter (λ) (non-stimulated)	0.5767 /s	Current paper
EC cell 5HT release amount	17935 molecules/release event	Current paper
5HT diffusion coefficient (D) – free fluid	5.4×10^{-6} cm^2/s	(Gerhardt and Adams, 1982)
5HT diffusion coefficient (D) – effective tissue	1.9810^{-6} cm^2/s	(Rice and Nicholson, 1986) (See text for comment)
Contraction model – contraction time	88 s	(Spencer et al., 2011)
SERT K_m	605 nM	(Miller et al., 2001)
SERT V_{max}	38 pmol/min/10^6 cells	(Miller et al., 2001)

Table 1: The various parameters used to create our models simulating the diffusion of 5-HT released form EC cells throughout the surround mucosa.

	GP EC cells (5-HT)	Human EC cells (5-HT)	Chromaffin cells (adrenaline)	Synapses (dopamine)*
Vesicle diameter (range, nm)	100-500**	-	100-500	20-50
Molecules released per vesicle	9,031 ± 354	9,642 ± 337	~700,000	~10,000
Amplitude (pA)	37.9 ± 1.1	49.1 ± 1.6	~80	~35
Half-width (µs)	96 ± 0.4	95 ± 0.4	~3000	~90
Rise time (µs)	27 ± 0.1	27± 0.1	~450	-

Table 2: Amperometric recordings reveal that EC cell release kinetics resembles that in synapses rather than in other endocrine cells. Amperometric measurements of single vesicle release of 5-HT from EC cells, adrenaline from chromaffin cells and dopamine from ventral midbrain neurons. The amount of EC cell 5-HT released per vesicle is over 70 times less than catecholamine released from similarly-sized vesicles in chromaffin cells (Keating et al., 2008). *Dopamine data are from (Staal et al., 2004). **Vesicle diameter measurements taken from (Nilsson et al., 1987; Cetin et al., 1994; Fujimiya et al., 1997) for EC cells, (Staal et al., 2004) for dopaminergic vesicles and (Pothos et al., 2002) for chromaffin cells.

Figure Legends:

Figure 1: Isolation and purification of primary EC cells. Low magnification of EC cells in culture labelled with a 5-HT antibody and viewed under **(A)** brightfield and **(B)** immunofluorescence. Red arrows illustrate 5-HT staining in these cells. **(C)** Cells staining positively for both 5-HT and the nuclear marker DAPI demonstrates >98% pure EC cell culture (n=3 cultures, ***p<0.001). **(D)** Higher magnification of these cells using confocal microscopy observed in brightfield (*top left*), the nuclear stain DAPI (blue), punctuate cytoplasmic 5-HT immunoreactivity (red) and the merged image. Scale = 8μm. **(E)** these cells also contain the EC cell marker, Tph1. Scale = 5μm. **(F)** Viability assay demonstrates cells are healthy in culture (n=4 cell cultures).

Figure 2: Stimulation of primary EC cells causes Ca^{2+} entry and 5-HT release. **(A)** Ca^{2+} currents elicited from -80mV holding potential, stepped for 100ms to -20mV to +30mV in 10mV increments. **(B)** current density-voltage relationship of these Ca^{2+} currents (n=6). **(C)** Example trace of Ca^{2+} entry in a single cell stimulated with 70mM K^+ (dashed line, Scale = 10 sec and 5 fluorescence points). (*Inset*) Average EC cell fluorescence change in response to 70mM K^+ or acetylcholine (ACh, 10μM, n=13 cells for both groups). **(D)** Amperometry measures 5-HT release from single EC cells. 70 mM K^+ solution (*dashed line*) triggers 5-HT release from single vesicles as indicated by individual current spikes. **(E)** (*Inset*) Oxidation current in 5-HT (10μM) when voltage is ramped from 0 to 0.8V using cyclic voltammetry demonstrates +400mV as the peak oxidation current for 5-HT. Scale bar = 100pA. Cells treated for 24 hours with the Tph inhibitor, LPS533401 (1μM) have almost no 5-HT release and

(F) this decrease is significant (***p<0.001, n=9-12 cells). Scale bar in C represents 100 pA and 20 sec in C and D.

Figure 3: EC cell 5-HT release is dependent on external Ca^{2+} entry via voltage gated Ca^{2+} channels. 70 mM K^+ (*dashed line*) triggers 5-HT release **(A)** in the presence of external Ca^{2+} and **(B)** in the same cell when external Ca^{2+} is removed. **(C)** A similar effect is seen in cells exposed to the L-type Ca^{2+} channel antagonist, nicardipine (2μM). Scale bars in A = 20 pA and 10 sec in A, B and C. **(D)** Quantification of spike frequency demonstrates that 70mM K^+ (n=18 paired recordings, *p<0.05) and acetylcholine (ACh, n=16 paired recordings, **p<0.01) increase the number of 5-HT release events and high K^+-induced release is reduced in the absence of external Ca^{2+} (n=6 paired recordings, **p<0.01) or presence of nicardipine (n=8 paired recordings, **p<0.01).

Figure 4: EC cell 5-HT release occurs with synaptic-like release kinetics. **(A)** Individual release events from EC cells are more rapid than those in **(B)** adrenal chromaffin cells. **(C)** A comparison of spike area distribution illustrates that the amount of EC cell 5-HT released per fusion event represents a separate population to release events from chromaffin cells. Faster release kinetics in EC cells are further illustrated by comparing the frequency distribution of spike **(D)** half-width, **(E)** rise time or **(F)** decay time in both cell types. n=2113 spikes from 24 EC cell recordings and 781 spikes from 16 chromaffin cell recordings.

Figure 5: Human EC cells also release 5-HT with synaptic kinetics. **(A)** An amperometric recording from a human EC cell in response to 70 mM K^+ (*dashed line*) exposure. Scale bar = 20 pA and 10 sec. **(B)** Average spike frequency is significantly increased by stimulation (n=21 cells from 4 cultures, ***p<0.001). **(C)** Relative number of events over time is similar in human and guinea pig EC cells stimulated by 70 mM K^+ while lack of external Ca^{2+} or L-type Ca^{2+} channel block similarly reduce cumulative spike frequency. **(D)** Single amperometric spikes from human EC cells have rapid kinetics. **(E)** The distribution of spike area ($Q^{1/3}$) in human cells (n=1542 spikes from 21 recordings, red) is the same as that in guinea pig cells (n=2113 spikes from 24 recordings, black). **(F)** Reducing 5-HT availability by treatment of guinea-pig EC cells with the Tph inhibitor LPS533401 (1μM) does not affect the amount of 5-HT released per vesicle.

Figure 6: Simulated 5-HT diffusion in the GI tract mucosal layer. EC cells 5-HT immunoreactivity in six representative regions of the guinea pig GI tract including the **(A)** oesophagus, **(B)** cardia, **(C)** fundus, **(D)** pylorus, **(E)** ileum and **(F)** colon. L= Lumen, S= Serosa, MM= Muscularis Mucosa; Scale bar 30 μm. **(G)** Average density of EC cells in various sections of the GI tract. **(H)** Diffusion of 5-HT after release from a single EC cell in stimulated and unstimulated conditions (n=6 simulations). **(I)** Effect of stimulation on the evolution of steady state 5-HT concentration (from starting point of 0mM) in different gut regions. **(J)** 3-dimensional, **(K)** z-plane and **(L)** x-y plane images of modeled steady state 5-HT concentrations in the pylorus (scale bar in L is for both K and L). **(M)** Average steady state 5-HT concentrations in different gut regions (n=5 simulations). **(N)** Proportion of cells in different regions exposed to an average 5-HT concentration >1 nM (n=5 simulations). **(O)** Model of

contraction-induced alterations in average 5-HT level (black) and proportion of cells exposed to >1 nM 5-HT (blue) in the ileum. **(P)** Increasing contraction frequency will ultimately lead to constant average 5-HT levels >1 nM and a higher proportion of cells exposed to >1 nM 5-HT.

Movie 1: Effect of stimulation on 5-HT levels (from starting point of zero) in the ileum mucosa over time. *Clockwise from top left*: Mean 5-HT concentration across the mucosal layer, 3-dimensional representation of 5-HT concentrations, x-y plane and z plane.

Movie 2: Effect of contraction on 5-HT levels (from starting point of zero) in the ileum mucosa over time under basal contraction rates. *Clockwise from top left*: Mean 5-HT concentration across the mucosal layer, 3-dimensional representation of 5-HT concentrations, x-y plane and z plane.

Movie 3: Effect of contraction on 5-HT levels (from starting point of zero) in the ileum mucosa over time under increased contraction rates. *Clockwise from top left*: Mean 5-HT concentration across the mucosal layer, 3-dimensional representation of 5-HT concentrations, x-y plane and z plane.

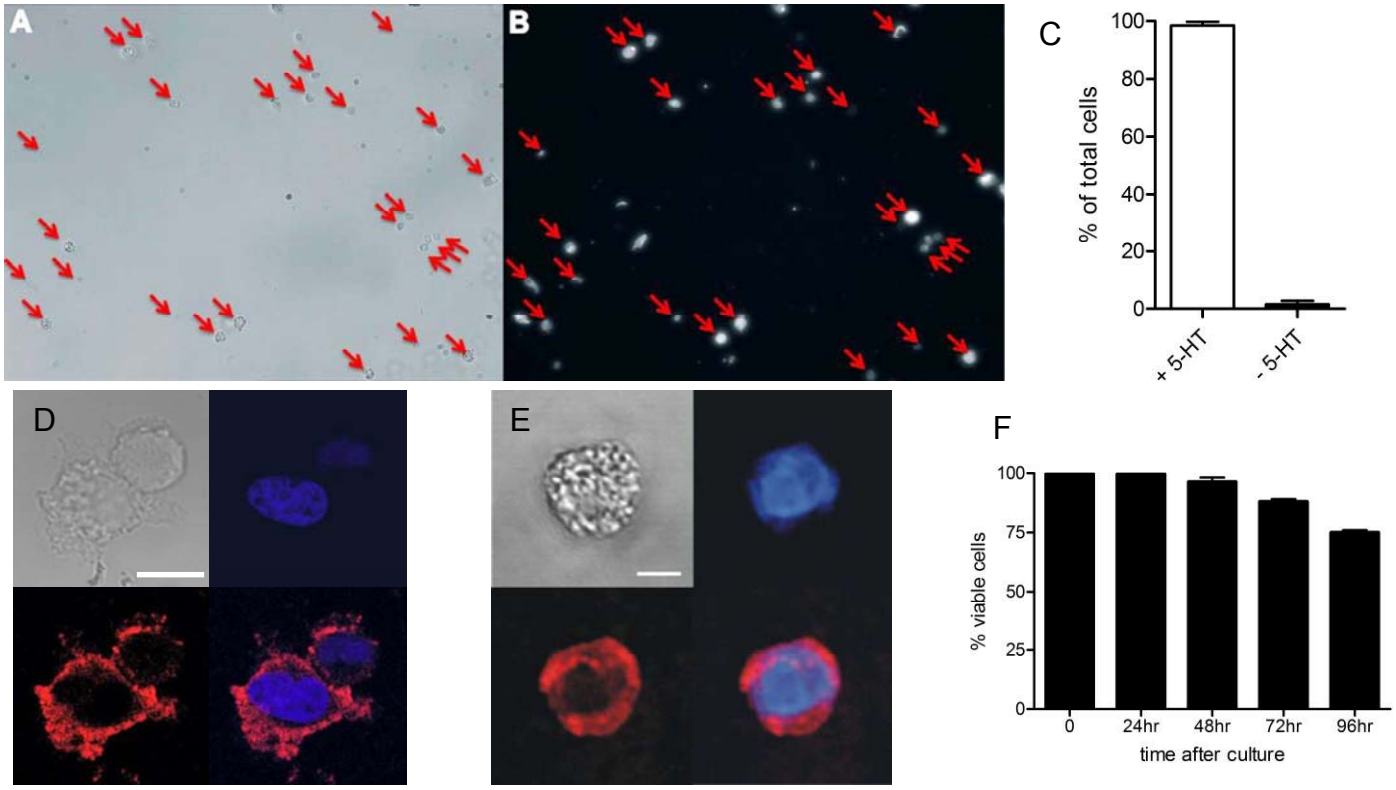
A
B
C
100
80
60
40
20
0
% of total cells
+ 5-HT
- 5-HT
D
E
F
100
75
50
25
0
% viable cells
0
24hr
48hr
72hr
96hr
time after culture

Figure 1

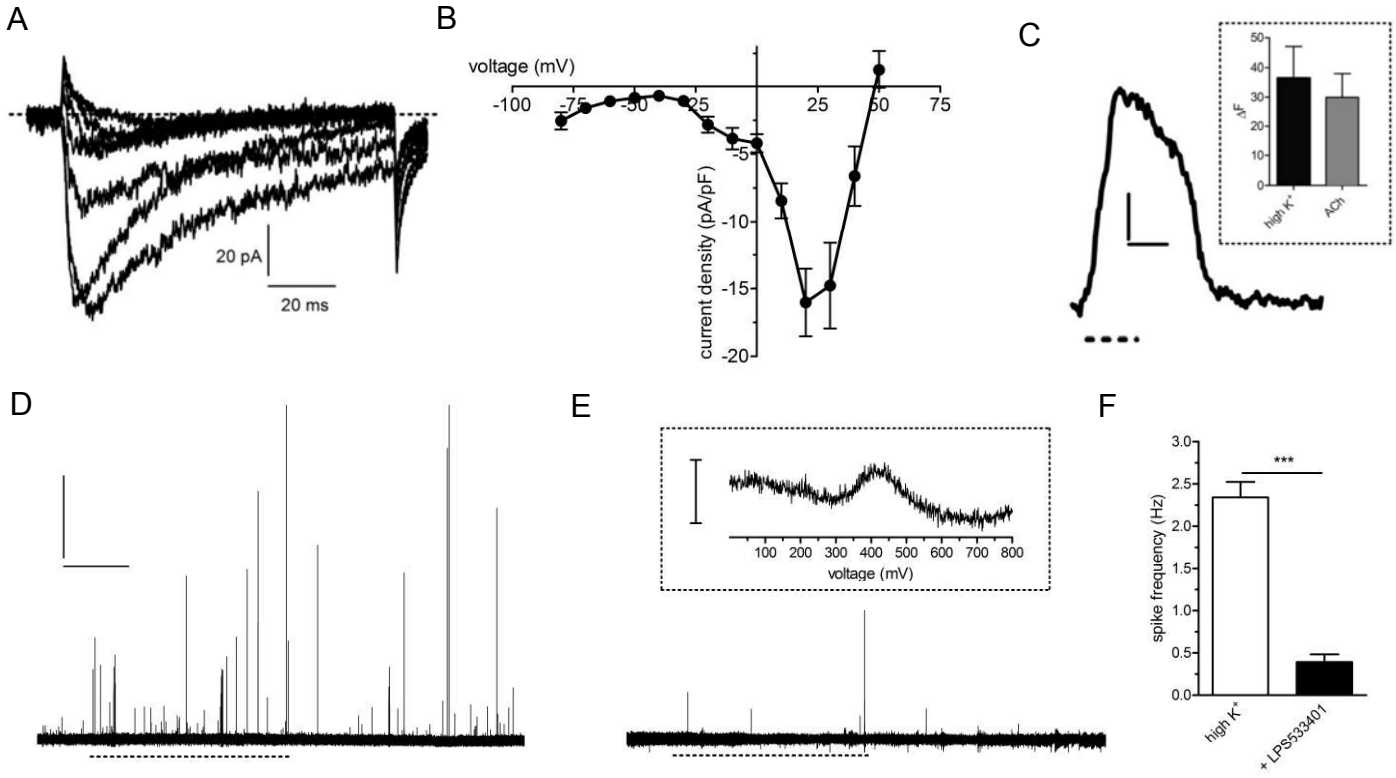
A
20 pA
20 ms
B
voltage (mV)
-100
-75
-50
25
50
75
-5
-10
-15
-20
current density (pA/pF)
C
ΔF
50
40
30
20
10
0
high K+
ACh
D
E
100 200 300 400 500 600 700 800
voltage (mV)
F
spike frequency (Hz)
3.0
2.5
2.0
1.5
1.0
0.5
0.0
***
high K+
+ LPS533401

Figure 2

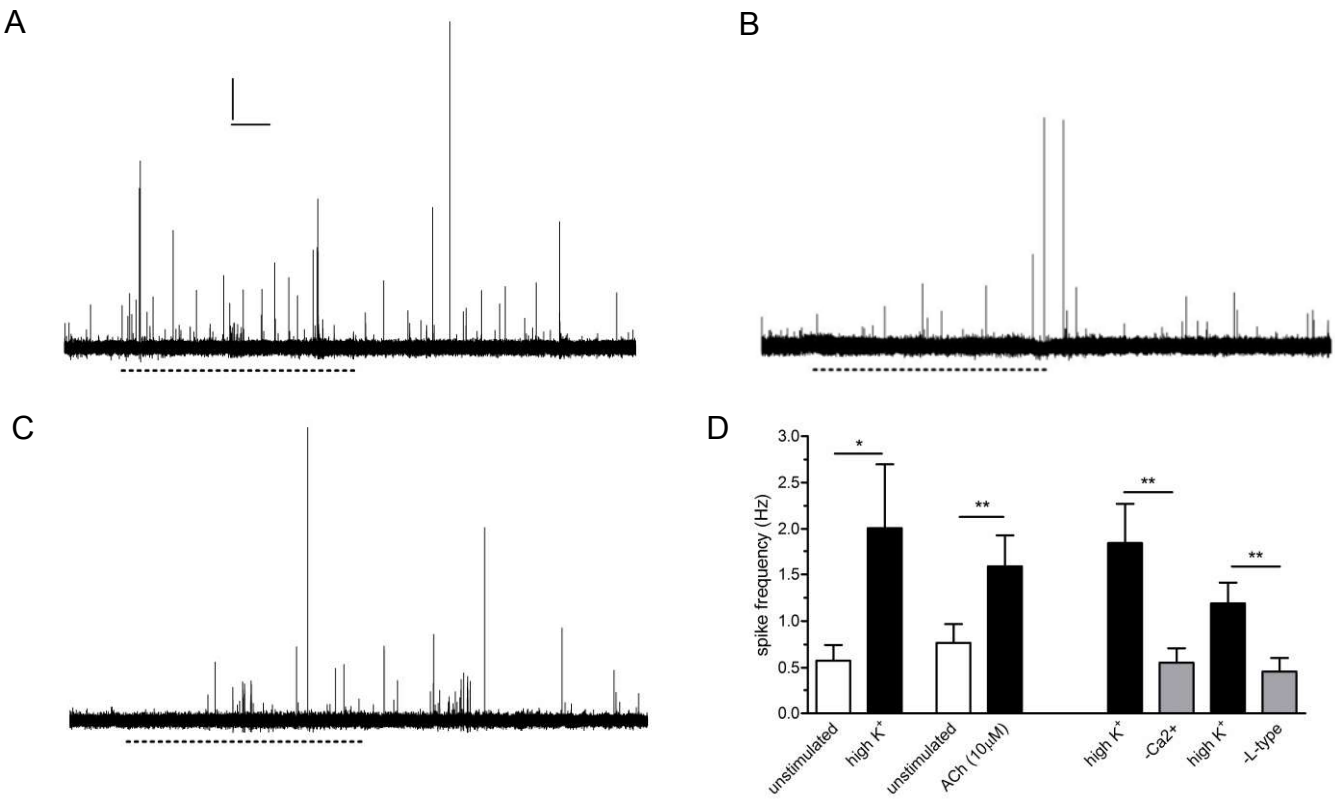
A
B
C
D
spike frequency (Hz)
3.0
2.5
2.0
1.5
1.0
0.5
0.0
*
**
**
**
unstimulated
high K+
unstimulated
ACh (10μM)
high K+
-Ca2+
high K+
-L-type

Figure 3

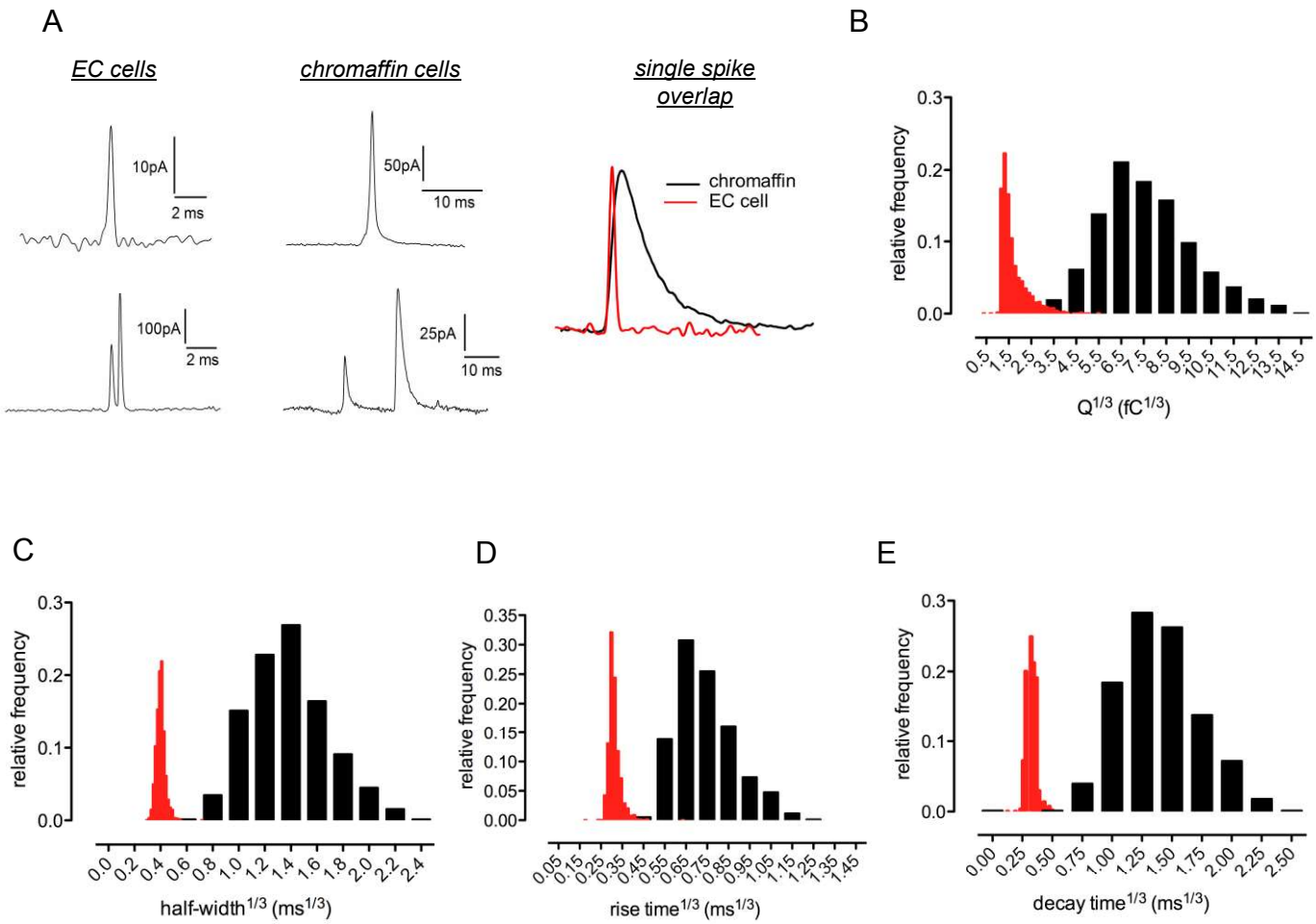
A
EC cells
chromaffin cells
single spike overlap
10pA
2 ms
100pA
2 ms
50pA
10 ms
25pA
10 ms
chromaffin
EC cell
B
relative frequency
Q1/3 (fC1/3)
C
relative frequency
half-width1/3 (ms1/3)
D
relative frequency
rise time1/3 (ms1/3)
E
relative frequency
decay time1/3 (ms1/3)

Figure 4

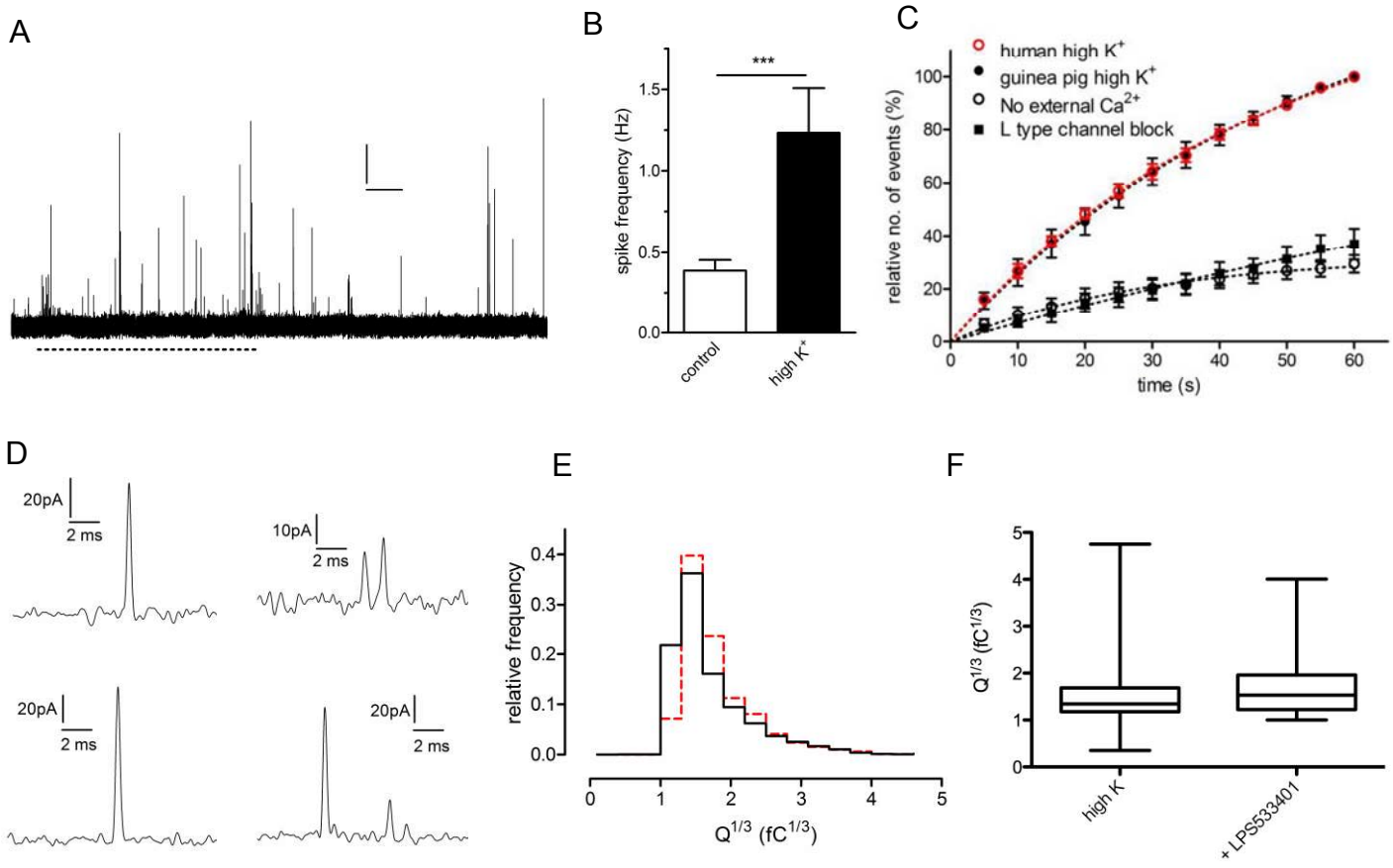
A
B
***
spike frequency (Hz)
control
high K+
C
human high K+
guinea pig high K+
No external Ca2+
L type channel block
relative no. of events (%)
time (s)
D
20pA
2 ms
10pA
2 ms
20pA
2 ms
20pA
2 ms
E
relative frequency
Q1/3 (fC1/3)
F
Q1/3 (fC1/3)
high K
+ LPS533401

Figure 5

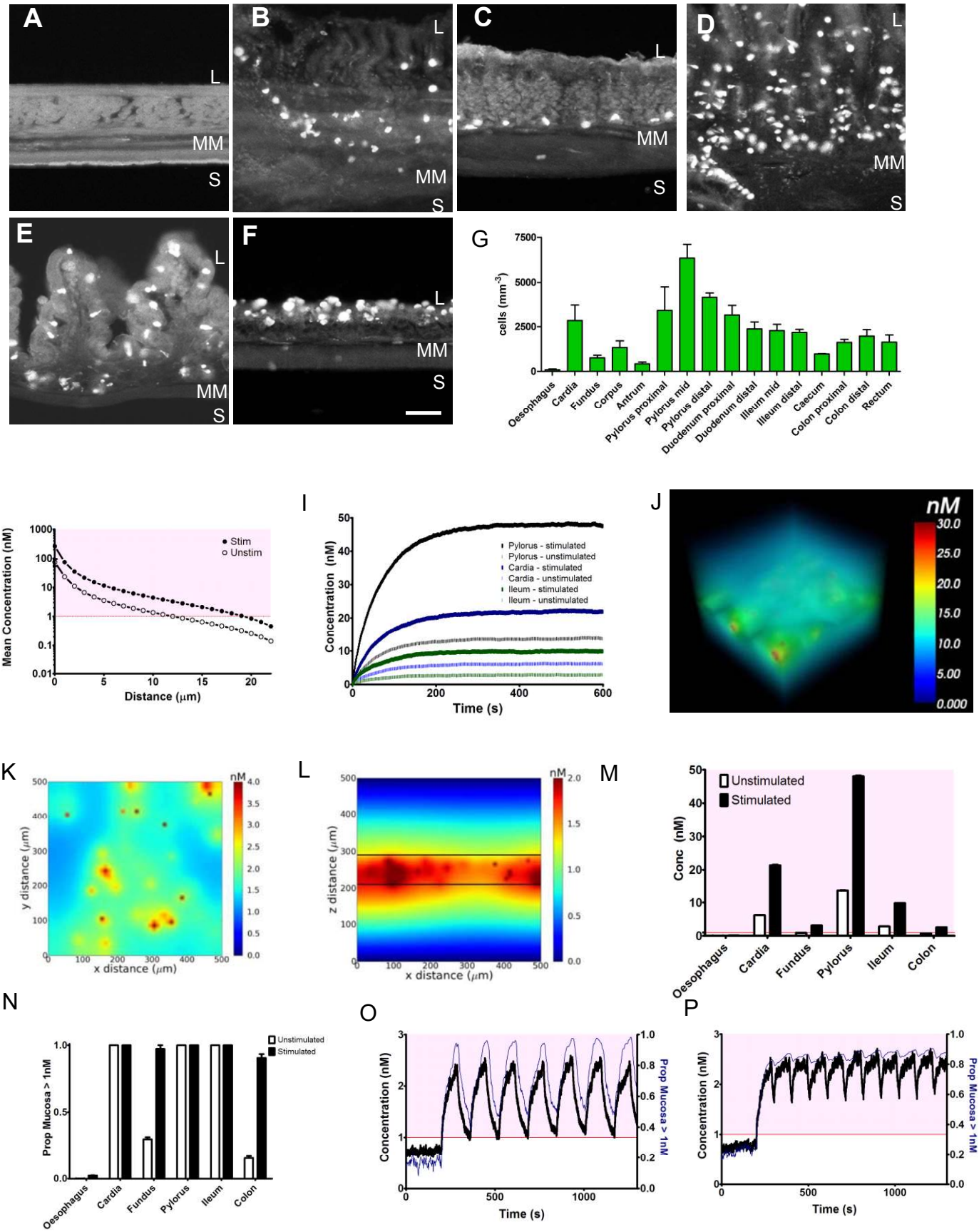
A
L
MM
S
B
L
MM
S
C
L
MM
S
D
L
MM
S
E
L
MM
S
F
L
MM
S
G
cells (mm-3)
7500
5000
2500
0
Oesophagus
Cardia
Fundus
Corpus
Antrum
Pylorus proximal
Pylorus mid
Pylorus distal
Duodenum proximal
Duodenum distal
Ileum mid
Ileum distal
Caecum
Colon proximal
Colon distal
Rectum
H
Mean Concentration (nM)
Stim
Unstim
Distance (μm)
I
Concentration (nM)
Pylorus - stimulated
Pylorus - unstimulated
Cardia - stimulated
Cardia - unstimulated
Ileum - stimulated
Ileum - unstimulated
Time (s)
J
nM
30.0
25.0
20.0
15.0
10.0
5.00
0.000
K
nM
y distance (μm)
x distance (μm)
L
nM
z distance (μm)
x distance (μm)
M
Unstimulated
Stimulated
Conc (nM)
Oesophagus
Cardia
Fundus
Pylorus
Ileum
Colon
N
Unstimulated
Stimulated
Prop Mucosa > 1nM
Oesophagus
Cardia
Fundus
Pylorus
Ileum
Colon
O
Concentration (nM)
Prop Mucosa > 1nM
Time (s)
P
Concentration (nM)
Prop Mucosa > 1nM
Time (s)

Figure 6

	GP EC cells (5-HT)	Human EC cells (5-HT)	Chromaffin cells (adrenaline)	Synapses (dopamine)*
Vesicle diameter (range, nm)	100-500**	-	100-500	20-50
Molecules released per vesicle	9,031 ± 354	9,642 ± 337	~700,000	~10,000
Amplitude (pA)	37.9 ± 1.1	49.1 ± 1.6	~80	~35
Half-width (μs)	96 ± 0.4	95 ± 0.4	~3000	~90
Rise time (μs)	27 ± 0.1	27± 0.1	~450	-

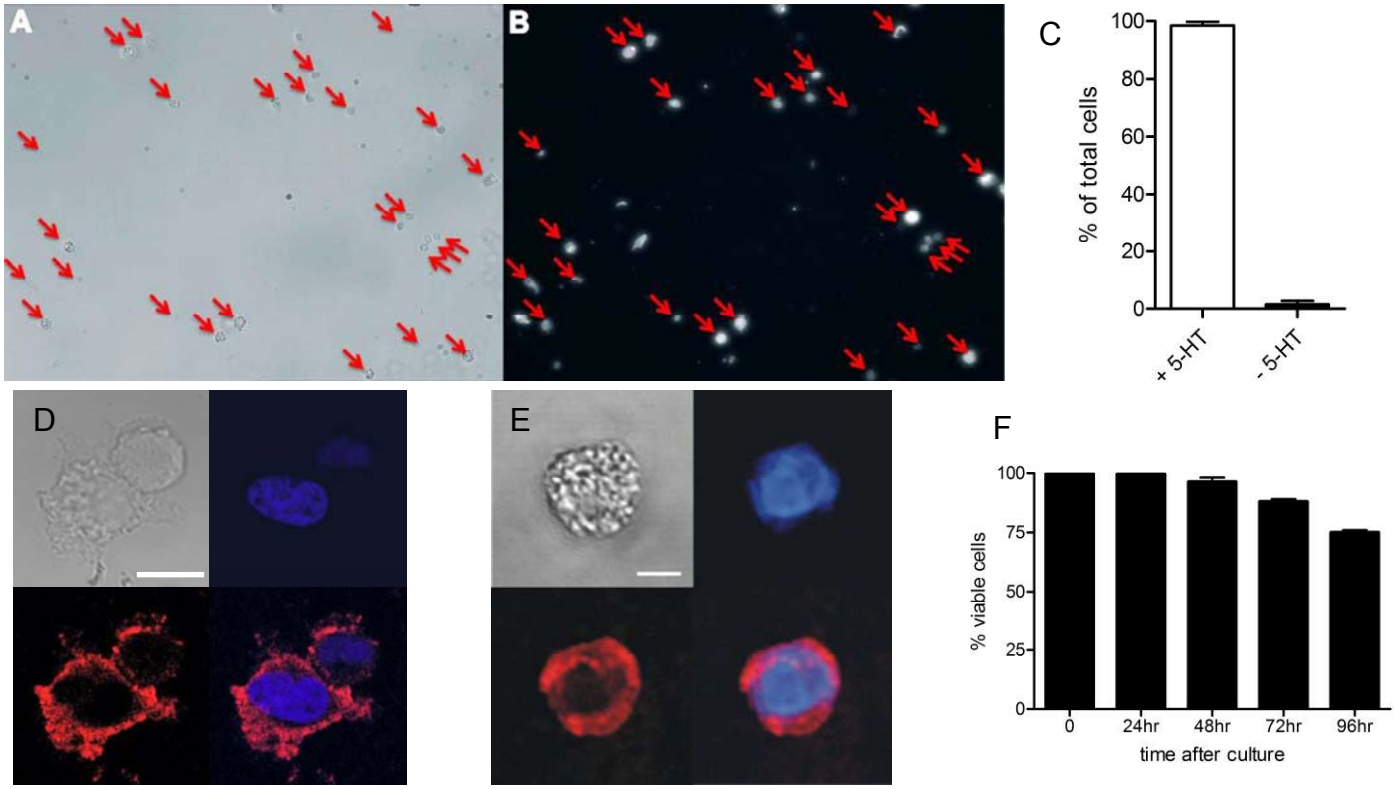
A
B
C
100
80
60
40
20
0
% of total cells
+ 5-HT
- 5-HT
D
E
F
100
75
50
25
0
% viable cells
0
24hr
48hr
72hr
96hr
time after culture

Figure 1

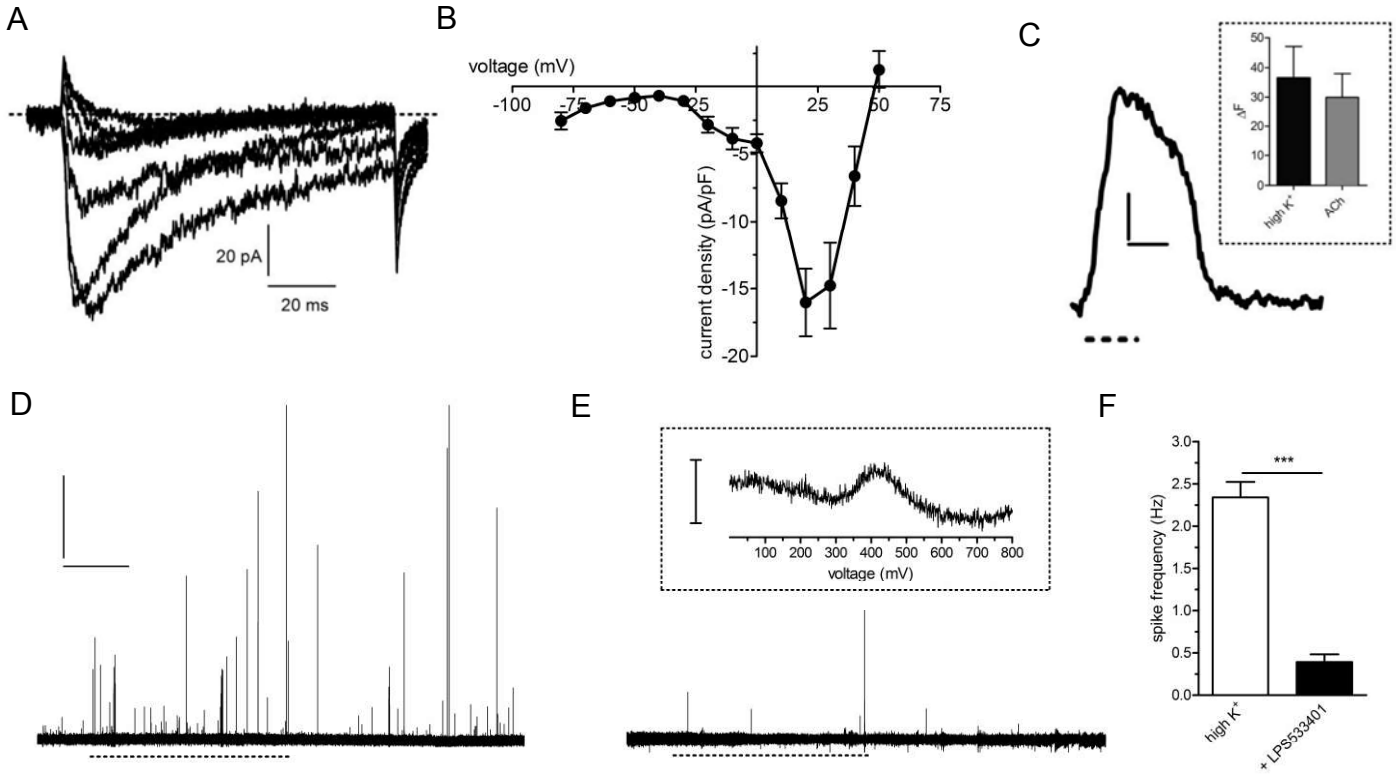
A
20 pA
20 ms
B
voltage (mV)
-100
-75
-50
25
50
75
-5
-10
-15
-20
current density (pA/pF)
C
ΔF
50
40
30
20
10
0
high K+
ACh
D
E
100 200 300 400 500 600 700 800
voltage (mV)
F
spike frequency (Hz)
3.0
2.5
2.0
1.5
1.0
0.5
0.0
***
high K+
+ LPS533401

Figure 2

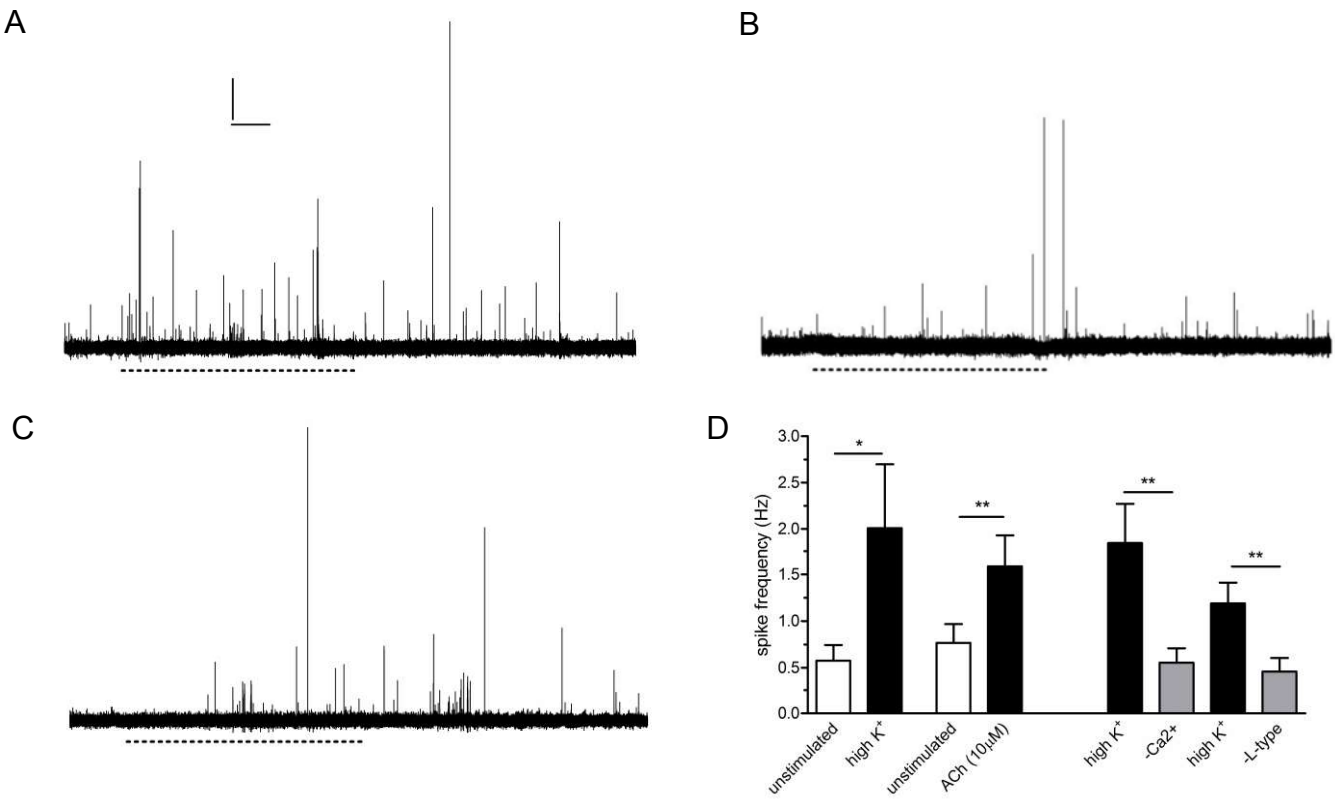
A
B
C
D
spike frequency (Hz)
3.0
2.5
2.0
1.5
1.0
0.5
0.0
*
**
**
**
unstimulated
high K+
unstimulated
ACh (10μM)
high K+
-Ca2+
high K+
-L-type

Figure 3

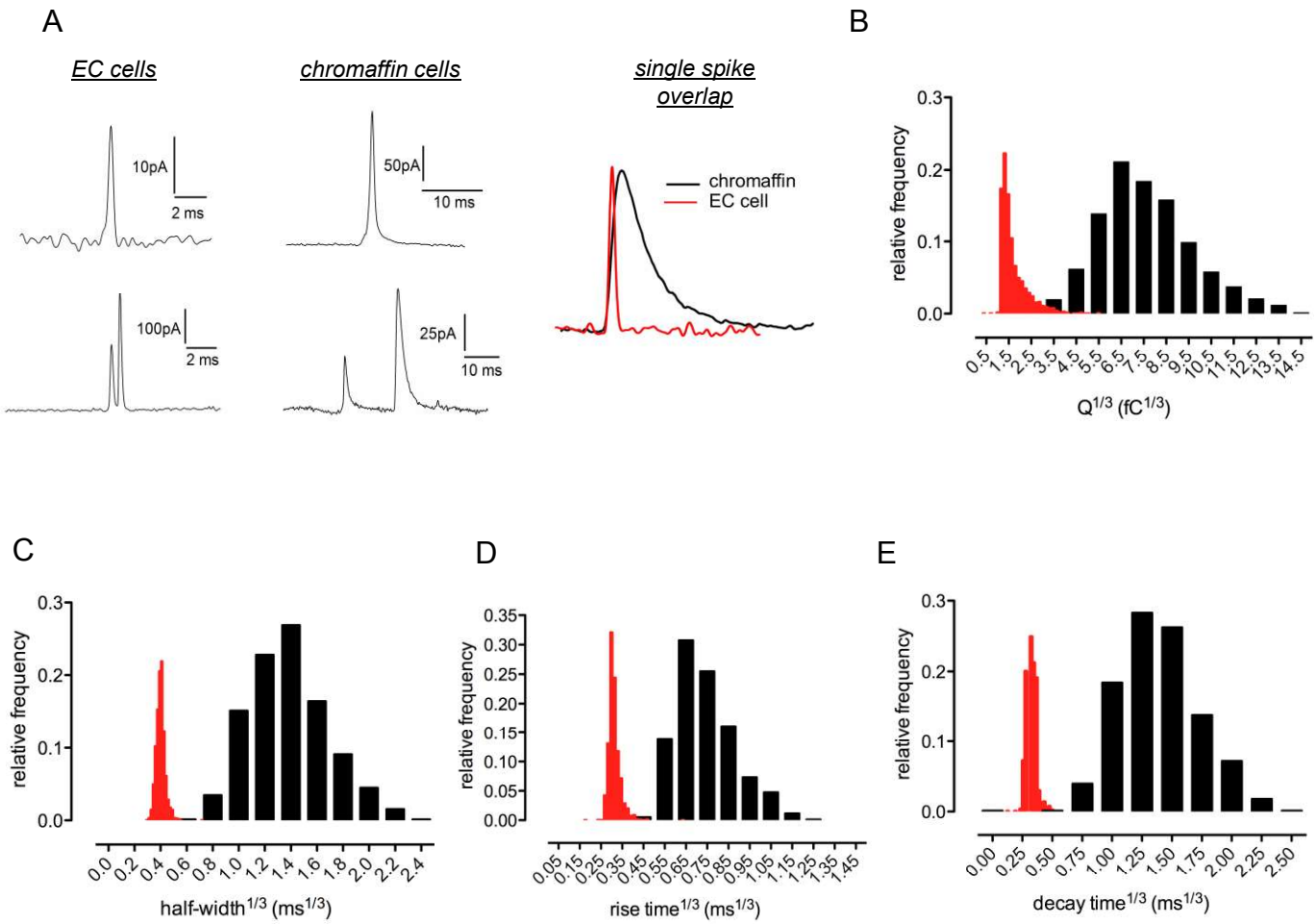
A
EC cells
chromaffin cells
single spike overlap
10pA
2 ms
100pA
2 ms
50pA
10 ms
25pA
10 ms
chromaffin
EC cell
B
relative frequency
Q1/3 (fC1/3)
C
relative frequency
half-width1/3 (ms1/3)
D
relative frequency
rise time1/3 (ms1/3)
E
relative frequency
decay time1/3 (ms1/3)

Figure 4

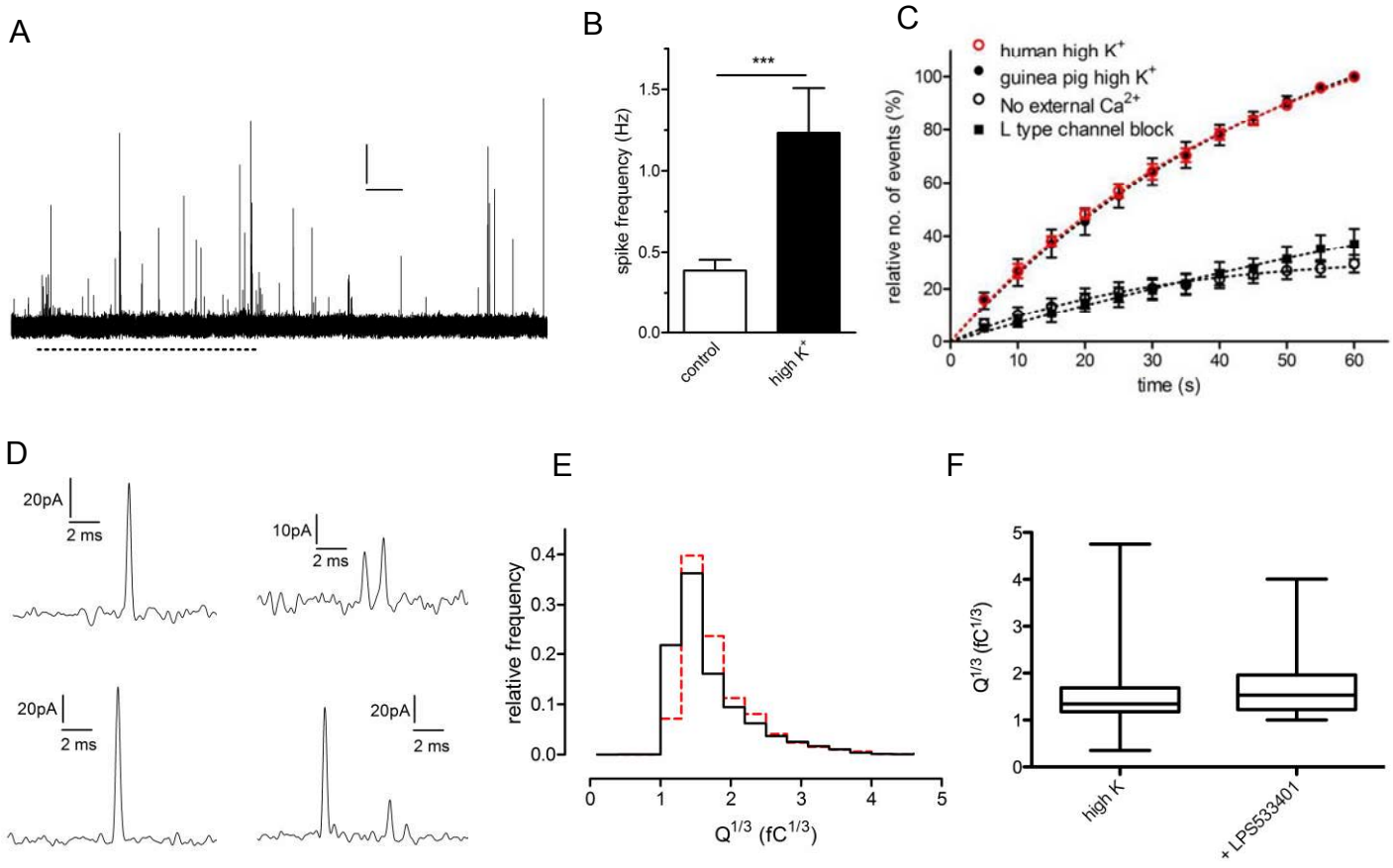
A
B
***
spike frequency (Hz)
control
high K+
C
human high K+
guinea pig high K+
No external Ca2+
L type channel block
relative no. of events (%)
time (s)
D
20pA
2 ms
10pA
2 ms
20pA
2 ms
20pA
2 ms
E
relative frequency
Q1/3 (fC1/3)
F
Q1/3 (fC1/3)
high K
+ LPS533401

Figure 5

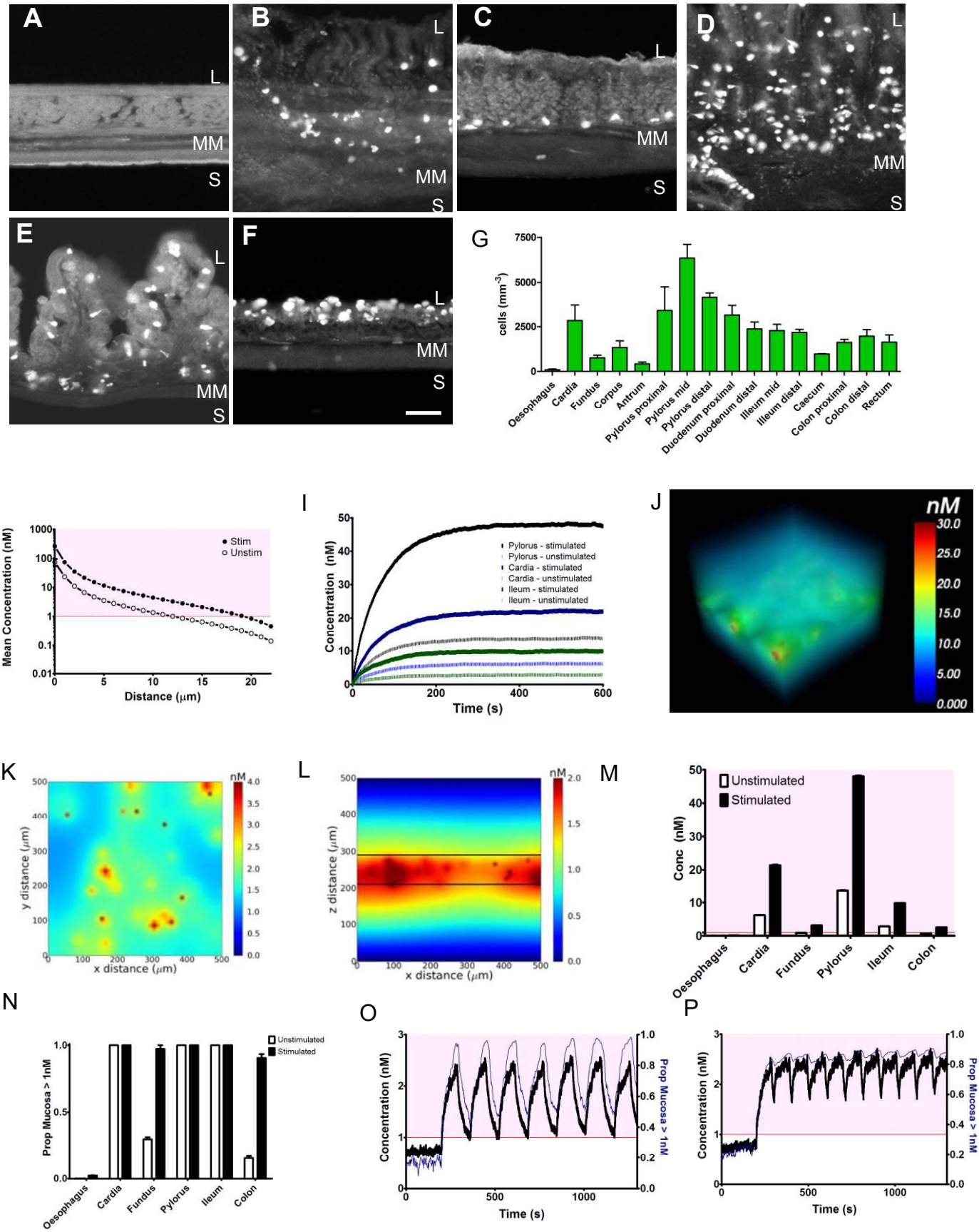
A
L
MM
S
B
L
MM
S
C
L
MM
S
D
L
MM
S
E
L
MM
S
F
L
MM
S
G
cells (mm-3)
7500
5000
2500
0
Oesophagus
Cardia
Fundus
Corpus
Antrum
Pylorus proximal
Pylorus mid
Pylorus distal
Duodenum proximal
Duodenum distal
Ileum mid
Ileum distal
Caecum
Colon proximal
Colon distal
Rectum
H
Mean Concentration (nM)
Stim
Unstim
Distance (μm)
I
Concentration (nM)
Pylorus - stimulated
Pylorus - unstimulated
Cardia - stimulated
Cardia - unstimulated
Ileum - stimulated
Ileum - unstimulated
Time (s)
J
nM
30.0
25.0
20.0
15.0
10.0
5.00
0.000
K
nM
y distance (μm)
x distance (μm)
L
nM
z distance (μm)
x distance (μm)
M
Unstimulated
Stimulated
Conc (nM)
Oesophagus
Cardia
Fundus
Pylorus
Ileum
Colon
N
Unstimulated
Stimulated
Prop Mucosa > 1nM
Oesophagus
Cardia
Fundus
Pylorus
Ileum
Colon
O
Concentration (nM)
Prop Mucosa > 1nM
Time (s)
P
Concentration (nM)
Prop Mucosa > 1nM
Time (s)

Figure 6

	GP EC cells (5-HT)	Human EC cells (5-HT)	Chromaffin cells (adrenaline)	Synapses (dopamine)*
Vesicle diameter (range, nm)	100-500**	-	100-500	20-50
Molecules released per vesicle	9,031 ± 354	9,642 ± 337	~700,000	~10,000
Amplitude (pA)	37.9 ± 1.1	49.1 ± 1.6	~80	~35
Half-width (μs)	96 ± 0.4	95 ± 0.4	~3000	~90
Rise time (μs)	27 ± 0.1	27± 0.1	~450	-